⌘ *Author's Choice*

THE JOURNAL OF BIOLOGICAL CHEMISTRY VOL. 292, NO. 12, pp. 5055–5069, March 24, 2017
© 2017 by The American Society for Biochemistry and Molecular Biology, Inc. Published in the U.S.A.

Decorin-inducible Peg3 Evokes Beclin 1-mediated Autophagy and Thrombospondin 1-mediated Angiostasis*

Received for publication, August 12, 2016, and in revised form, February 6, 2017 Published, JBC Papers in Press, February 7, 2017, DOI 10.1074/jbc.M116.753632

Annabel Torres[1], **Maria A. Gubbiotti, and Renato V. Iozzo**[2]

From the Department of Pathology, Anatomy, and Cell Biology and the Cancer Cell Biology and Signaling Program, Kimmel Cancer Center, Sidney Kimmel Medical College, Thomas Jefferson University, Philadelphia, Pennsylvania 19107

Edited by Amanda J. Fosang

We previously discovered that systemic delivery of decorin for treatment of breast carcinoma xenografts induces paternally expressed gene 3 (Peg3), an imprinted gene encoding a zinc finger transcription factor postulated to function as a tumor suppressor. Here we found that *de novo* expression of Peg3 increased Beclin 1 promoter activity and protein expression. This process required the full-length Peg3 as truncated mutants lacking either the N-terminal SCAN domain or the zinc fingers failed to translocate to the nucleus and promote Beclin 1 transcription. Importantly, overexpression of Peg3 in endothelial cells stimulated autophagy and concurrently inhibited endothelial cell migration and evasion from a 3D matrix. Mechanistically, we found that Peg3 induced the secretion of the powerful angiostatic glycoprotein Thrombospondin 1 independently of Beclin 1 transcriptional induction. Thus, we provide a new mechanism whereby Peg3 can simultaneously evoke autophagy in endothelial cells and attenuate angiogenesis.

Paternally expressed gene 3 (Peg3)[3] was recently identified in our laboratory as a gene induced in the stroma of breast carcinoma xenografts following systemic delivery of decorin (1), a small leucine-rich proteoglycan with antioncogenic and antiangiogenic properties (2–4). We subsequently discovered that Peg3 is essential for decorin-induced autophagy in endothelial cells (5, 6) and that decorin expression is induced both *in vitro* and *in vivo* by proautophagic stimuli like starvation and mammalian target of rapamycin (mTOR) inhibition (7, 8). Furthermore, Peg3 is also necessary for the induction of endothelial cell autophagy evoked by another matrix constituent, endorepellin (9, 10), the C-terminal fragment of perlecan previously implicated in angiostasis (11–15). Together, these studies show that Peg3 is an important link between soluble matrix molecules and their regulation of a vital cellular process, autophagy (16). However, the precise mechanism of Peg3-evoked autophagy in endothelial cells remains unknown.

Structurally, Peg3, one of only ~79 imprinted genes in the human genome (17, 18), harbors an N-terminal SCAN domain, which functions as a protein-protein interaction motif allowing Peg3 to homo- or heterodimerize, and an extended C terminus containing 12 C_2H_2 Krüppel-like zinc finger domains capable of binding DNA (19–21). Functionally, Peg3 has been implicated in several cellular processes involved in cell growth and development. During gastrulation, Peg3 is first detected in the ectoderm and mesoderm with strong expression in extraembryonic tissues (22). In adult tissues, Peg3 is ubiquitously expressed with the highest levels in brain, skeletal muscle, testis, and ovary (22). In skeletal muscle, the interaction of Peg3 with tumor necrosis factor (TNF) receptor-associated factor 2 induces NFκB nuclear translocation (23) and inhibits myogenesis, leading to cachexia (24). This interaction occurs in a subpopulation of interstitial stem cells where Peg3 modulates caspase activity in response to TNFα and contributes to the loss of muscle regeneration (25). Peg3 expression is also considered a stem cell marker in the epidermis, small intestine, and central nervous system (26). Peg3 promotes apoptosis downstream of p53/c-Myc by associating with Siah1a (Seven in absentia homolog 1a) and stimulating Bax translocation from the cytosol to the mitochondrial outer membrane for the release of cytochrome *c* (27, 28). The apoptotic function of Peg3 is activated in neuronal cells during hypoxia (29). In this cell type, Peg3 is primarily expressed in the nucleus and upon induction affects gene transcription, which in turn stimulates Bax translocation (30).

In agreement with the high expression of Peg3 in the brain and its role in development, $Peg3^{-/-}$ mice display abnormal behavior and metabolic disorders (31, 32). Female $Peg3^{-/-}$ mice exhibit atypical nurturing behavior, and the pups have stunted growth and impaired suckling, leading to decreased survival (32). Conversely, despite the reduction in nutrient intake, these mice have increased body fat, which may be due to the ability of Peg3 to modulate genes involved in lipid metabolism and adipocyte differentiation (33). However, a recent

* This work was supported in part by National Institutes of Health Grants RO1 CA39481, RO1 CA47282, and RO1 CA164462 (to R. V. I.). The authors declare that they have no conflicts of interest with the contents of this article. The content is solely the responsibility of the authors and does not necessarily represent the official views of the National Institutes of Health.
⌘ *Author's Choice*—Final version free via Creative Commons CC-BY license.
[1] Supported by a Diversity Research Supplement, National Institutes of Health Grant CA39481-26S1. This work is a partial fulfillment of a doctoral thesis in Cell and Developmental Biology, Thomas Jefferson University.
[2] To whom correspondence should be addressed: Dept. of Pathology, Anatomy and Cell Biology, Thomas Jefferson University, 1020 Locust St., Suite 336 JAH, Philadelphia, PA 19107. Tel.: 215-503-2208; E-mail: renato.iozzo@jefferson.edu.

[3] The abbreviations used are: Peg3, paternally expressed gene 3; AMPK, adenosine monophosphate-activated protein kinase; HUVEC, human umbilical vein endothelial cell; LC3, microtubule-associated light chain 3; mTOR, mammalian target of rapamycin; VEGFR2, vascular endothelial growth factor receptor 2; PAER2 cells, porcine aortic endothelial cells stably expressing VEGFR2; ZF, zinc finger domains; TSP-1, Thrombospondin 1; rh, recombinant human; BECN1, Beclin 1; MTT, 3-(4,5-dimethylthiazol-2-yl)-5-(3-carboxymethoxyphenyl)-2-(4-sulfophenyl)-2*H*-tetrazolium.

report has provided evidence against a role of Peg3 in maternal care but favors a more general function for Peg3 in regulating body growth (34).

Unlike in normal Mendelian inheritance, imprinted genes are only expressed by either the maternal or paternal allele as the other is silenced via histone alterations and/or promoter methylation (35). Because only one allele is expressed, imprinting is important in the context of cancer as imprinted tumor suppressor genes are more vulnerable to loss of heterozygosity than genes expressed on both alleles. Unsurprisingly, loss of Peg3 due to hypermethylation of the promoter or loss of heterozygosity has been implicated in several malignancies (36–40). In fact, re-expression of Peg3 in ovarian and glioma cell lines suppresses tumorigenicity *in vitro* and *in vivo* (37, 41, 42). In glioma cell lines, reintroducing Peg3 abrogates Wnt signaling by promoting degradation of β-catenin via the proteasome in a non-canonical pathway that is independent of glycogen synthase kinase 3β (42). Intriguingly, this function of Peg3 appears functionally akin with that of decorin (43). These studies provide evidence that this imprinted gene may function as a *bona fide* tumor suppressor.

As mentioned above, we discovered a novel function for Peg3 as a key regulator of decorin-induced autophagy (5, 6). Decorin is primarily synthesized by fibroblasts, smooth muscle cells, and macrophages (44–47) and is involved in modulating several biological processes including collagen fibrillogenesis, bone and skin homeostasis, vertebrate convergent extension, myogenesis, cancer, and angiogenesis (48–64). Although decorin was initially thought to function as a collagen-binding proteoglycan and thus as a primary regulator of collagen fibrillogenesis (50, 65–69), recent evidence shows that decorin plays a much broader role in the modulation of cell signaling pathways via interactions with growth factors and several receptor tyrosine kinases (70). Decorin functions as a tumor repressor, inhibiting cancer growth, migration, and angiogenesis via downregulation of the oncogenes Myc, β-catenin (in a glycogen synthase kinase 3β-independent manner), and hypoxia-inducible factor 1, α subunit (43, 47, 71–74).

During the early stages of autophagic induction, decorin non-canonically activates the energy sensor kinase AMPK by promoting phosphorylation of the AMPKα subunit at Thr^{172} (6). Concurrently, decorin attenuates phosphorylation of critical antiautophagic effectors such as the serine/threonine-specific protein kinase Akt, mTOR, and p70S6K (6) downstream of vascular endothelial growth factor receptor 2 (VEGFR2) signaling. Similar to AMPK, Peg3 is essential for endothelial cell autophagy evoked by decorin and represents a novel regulator of autophagy (5). Silencing Peg3 with siRNA abrogates the ability of decorin to induce the autophagic gene *MAP1LC3A* and prevents induction of the Beclin 1 (*BECN1*) gene beyond basal levels (5). Interestingly, knockdown of Peg3 also reduces basal expression of *BECN1*, indicating that the two are closely linked (5).

In the present study, we investigated the role of Peg3 in autophagy and angiogenesis (75). We discovered that *de novo Peg3* expression enhanced Beclin 1 transcription and promoted endothelial cell autophagy. Constitutive expression of Peg3 also inhibited endothelial cell migration and evasion from a 3D matrix and evoked secretion of Thrombospondin 1, suggesting that endogenous levels of Peg3 could concurrently regulate both autophagy and angiogenesis.

Results

Peg3 Localizes to the Nucleus of PAER2 Cells—Peg3 is a putative DNA-binding protein due to its C_2H_2 zinc finger motifs (20, 22, 24, 30). Thus, to ascertain whether Peg3 behaves as a DNA-binding protein in endothelial cells, we elucidated its subcellular localization. We transiently transfected PAER2 cells, transgenic porcine aortic endothelial cells overexpressing VEGFR2, with hemagglutinin (HA)-tagged full-length Peg3 or deletion constructs containing either the N-terminal SCAN domain (PEG3-SCAN) or the zinc finger domains (PEG3-ZF) (Fig. 1*A*). The HA tag allowed us to specifically recognize transgenic Peg3 and its truncations. Using confocal microscopy, we found that only full-length Peg3 localized to the nucleus in contrast to both deletions, which remained within the cytoplasm (Fig. 1, *C–E*). Transfection with the empty vector showed no signal (Fig. 1*B*). To validate the presence of Peg3 in the nucleus, we utilized *z*-stack optical sections with *xz* orthogonal views where the yellow color confirms the presence of Peg3 in the nucleus. Line scanning was used to assess co-localization of the *green* fluorophore (Peg3) with the nuclear staining (*red*) as measured between the *white arrows*. Importantly, full-length Peg3 was the only condition where both channels superimposed, indicating co-localization of Peg3 and DNA (Fig. 1, *F–I*). These results were corroborated by biochemical cell fractionations, confirming that only full-length Peg3 was present in the nucleus (Fig. 1, *J–M*). These findings indicate that Peg3 is capable of entering the nucleus of PAER2 cells and co-localizing with DNA to potentially regulate transcription.

Endogenous Peg3 Localizes to the Nucleus following Autophagic Induction with Either Decorin or Rapamycin—To determine whether endogenous Peg3 localizes to the nucleus in response to autophagic induction, PAER2 cells were treated with decorin or rapamycin, an established mTOR inhibitor. Under basal conditions, endogenous Peg3 resided primarily in the cytoplasm (Fig. 2*A*), but it efficiently translocated into the nuclei following decorin or rapamycin treatment (Fig. 2, *B* and *C*). Furthermore, line scanning of the areas between the *white arrows* demonstrates co-localization of Peg3 with DNA (Fig. 2, *D–F*) only after autophagic stimulation. Biochemical data using cytoplasmic-nuclear fractionation further confirmed that Peg3 was virtually undetectable in the nucleus under basal conditions but translocated after treatment of decorin or rapamycin (Fig. 2, *G–I*). These data validate the presence of endogenous Peg3 in the nucleus upon autophagic activation.

Peg3 Evokes BECN1 Promoter Activity—To investigate whether Peg3 does indeed regulate *BECN1* promoter activity in PAER2 cells, we utilized a vector harboring a 1.4-kb promoter region (here referred to as full length) of the *BECN1* gene and a series of 5′ deletion constructs fused to the luciferase reporter gene (Fig. 3*A*). We identified three putative binding sites for Peg3 encompassing the core sequence (5′-TGGCT-3′) within the 1.4-kb region of the *BECN1* promoter (76, 77). We found that cells constitutively expressing Peg3 had a 2-fold increase in *BECN1* mRNA vis-à-vis normal counterparts, suggesting regu-

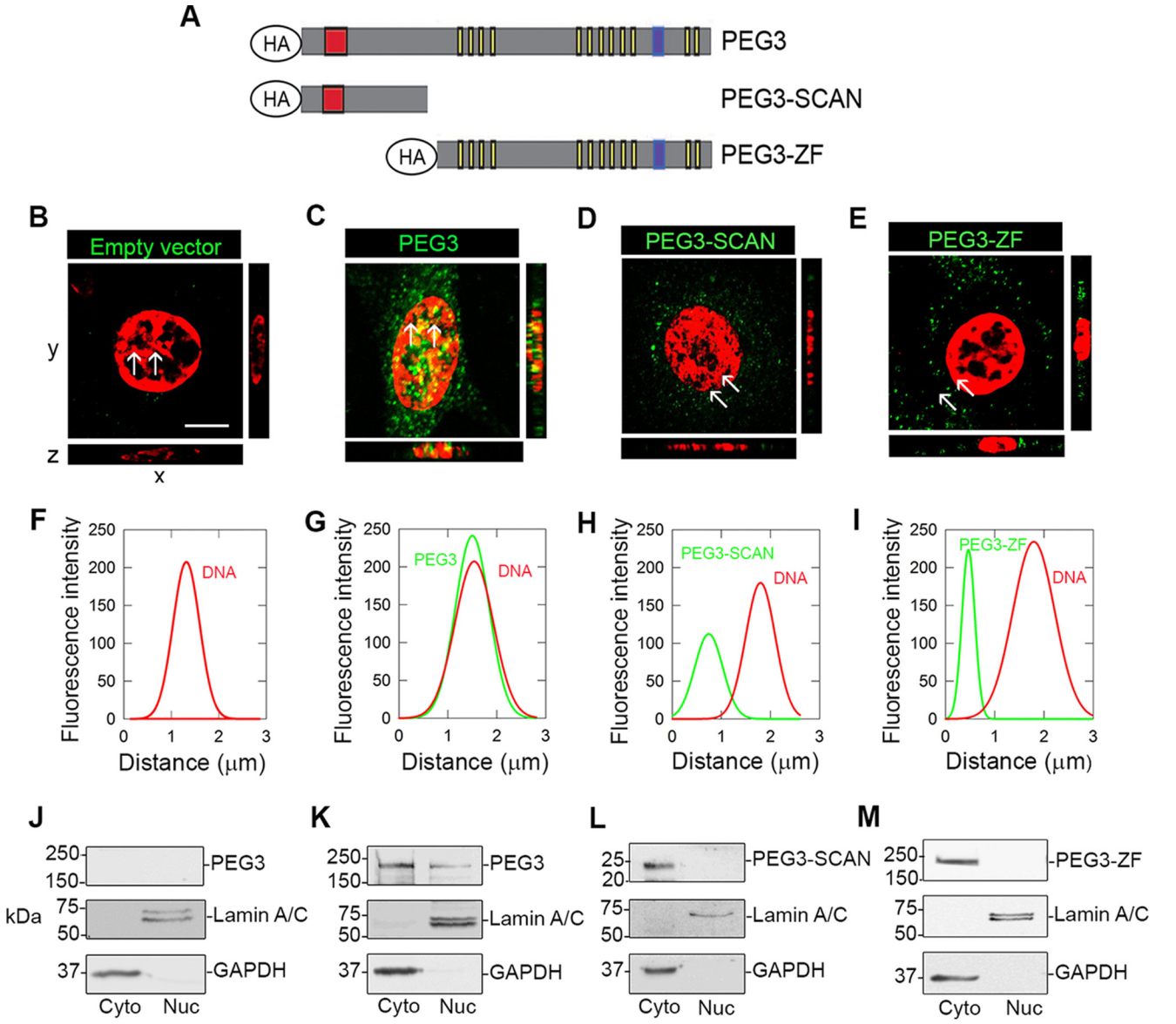

FIGURE 1. **Peg3 translocates to the nucleus and co-localizes with DNA.** *A*, constructs used for the overexpression of Peg3 and truncations containing either the N terminus and SCAN domain (PEG3-SCAN; *red box*) or C terminus and zinc finger domains (PEG3-ZF; *yellow boxes*). Peg3 also contains a proline-rich region in *blue*. *B–E*, confocal images of PAER2 cells following a 48-h transfection of Peg3 where an anti-HA antibody was used to detect Peg3 and its truncations (*green*). Nuclei were stained with DAPI to visualize DNA, and the color of the blue channel was changed to *red* for a more efficient visualization of the co-localization (*scale bar*, ~10 μm). *F–I*, line scan profiles corresponding to each confocal image displaying fluorescence distribution (pixels) measured between the *white arrows* for each channel. All images were captured using the same exposure, gain, and intensity. *J–M*, cytoplasmic (*Cyto*) and nuclear (*Nuc*) fractionations performed after 48-h transfections, validating Peg3 cellular localization.

lation of Beclin 1 by Peg3 at the level of transcription ($p < 0.01$; Fig. 3*B*). We then generated cell lines stably expressing luciferase driven by the *BECN1* promoter and then transiently transfected these cells with increasing concentrations of a Peg3-containing expression vector. Time course experiments revealed that transient transfection of Peg3 was optimal at 48 h for robust luciferase activity of the full-length *BECN1* promoter (Fig. 3*C*). Using the full-length promoter, luciferase induction was dose-dependent and saturable with an initial increase at ~100 ng and saturation occurring at ~600 ng (Fig. 3*D*, *red triangles*). In contrast, transient transfection with equimolar amounts of empty vector had no effect (Fig. 3*D*, *black triangles*). Additionally, Torin 1, an ATP-competitive inhibitor of mTOR (78), induced *BECN1* promoter activity to levels nearly comparable with those achieved by Peg3 overexpression, validating that our luciferase reporter system increases activity under proautophagic conditions ($p < 0.001$; Fig. 3*E*).

To identify the minimal region for induction of *BECN1* promoter activity by Peg3, we used the 5′ truncation mutants whereby each promoter truncation lacked one predicted Peg3-binding site. Peg3 was able to promote a significant induction at 600 ng in the Δ1 *BECN1*-luciferase stable cell line that contained two predicted Peg3-binding sites ($p < 0.001$; Fig. 3*F*). Interestingly, after the second Peg3-binding site was eliminated (Δ2), Peg3 had no effect on luciferase activity (Fig. 3*G*), similar to the elimination of all three Peg3-binding sites (Δ3; Fig. 3*H*).

Additionally, to determine whether Peg3 directly associates at these putative binding sites within the *BECN1* promoter, we

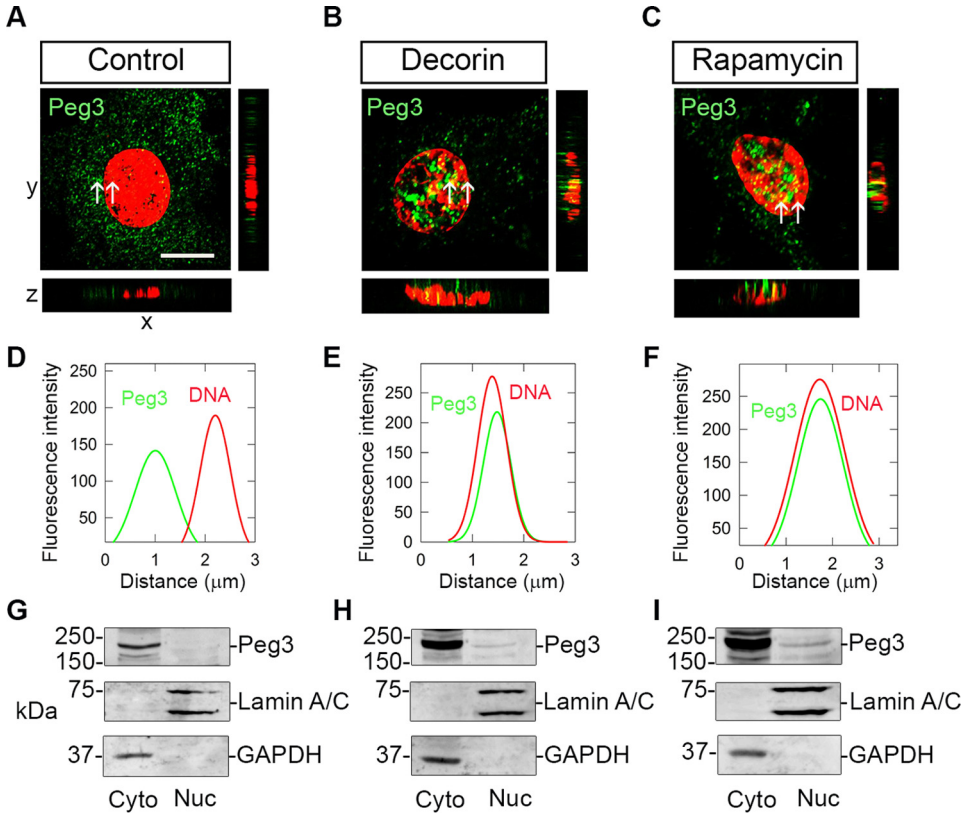

FIGURE 2. **Peg3 translocates to the nucleus following decorin- or rapamycin-induced autophagy.** *A–C*, confocal microscopy of endogenous Peg3 (*green*) present in the cytoplasm under basal conditions (*A*) and localized to the nucleus upon treatment with decorin (200 nM) (*B*) or rapamycin (40 nM) (*C*). Nuclei were stained with DAPI (false colored *red*) (*scale bar*, ~10 μm). *D–F*, line scanning between the *white arrows* indicating co-localization of Peg3 with DNA. All images were captured using the same exposure, gain, and intensity. *G–I* cytoplasmic (*Cyto*) and nuclear (*Nuc*) fractionations performed to validate Peg3 cellular localization after decorin and rapamycin treatment as compared with basal conditions.

generated a 1.4-kb *BECN1* promoter-luciferase construct incorporating nucleotide changes to the core Peg3 binding consensus site. The core sequence (5′-TGGCT-3′) of the Peg3-binding site was mutated to 5′-TAACC-3′ for all three potential binding sites. The point mutations were verified through Sanger sequencing (data not shown). Notably, the PAER2 cells stably expressing the promoter with mutant Peg3-binding sites did not respond to increasing concentrations of transfected Peg3 cDNA ($p > 0.05$; Fig. 3*I*). Collectively, these data indicate that Peg3 mediates *BECN1* transcription and that the minimal *BECN1* promoter region required for Peg3-dependent expression lies between −1407 and −645 bp.

De Novo Expression of Peg3 Increases Beclin 1 Protein Levels in Endothelial Cells—Next, we assessed the effect on endothelial Beclin 1 protein levels evoked by increasing concentrations of Peg3 cDNA. The level of transgenic HA-tagged Peg3 was directly proportional to the transfected Peg3 cDNA (Fig. 4*A*) in contrast to empty vector (Fig. 4*B*). Notably, the levels of Peg3 protein correlated with induction of Beclin 1 protein (Fig. 4, *A* and *C*). Next, PAER2$^{BECN1\text{-}Luc}$ cells were transiently transfected with increasing concentrations of the truncated Peg3 constructs PEG3-SCAN and PEG3-ZF. Both Peg3 deletions failed to induce luciferase activity (Fig. 4, *D* and *F*), which was expected because neither truncation was capable of nuclear translocation (Fig. 1, *D* and *E*). Furthermore, these results correlated with protein levels of Beclin 1, which also remained unchanged (Fig. 4, *E* and *G*). Thus, the entire Peg3 protein is necessary for *BECN1* transcriptional induction and consequent protein expression.

To further evaluate Peg3-mediated Beclin 1 expression, we generated endothelial cells stably expressing full-length Peg3, PAER2^{PEG3} (Fig. 4*H*), and found that basal levels of Beclin 1 were significantly up-regulated (Fig. 4*I*). We have previously shown that treatment of endothelial cells with decorin or rapamycin results in increased Beclin 1 protein expression (5). Interestingly, neither treatment further increased Beclin 1 levels in PAER2^{PEG3} (Fig. 4, *I* and *J*). These findings suggest that Beclin 1 expression levels in Peg3-overexpressing cells were already maximal and could not be further enhanced by either decorin or rapamycin.

Peg3 Overexpression Promotes Autophagic Flux—To determine whether *de novo* Peg3 expression enhances autophagic flux following the transcriptional induction of Beclin 1, we treated the PAER2^{PEG3} cells with bafilomycin A1. Bafilomycin A1 blocks the vacuolar (V-type) H^+-ATPase, thereby inhibiting autophagosomal fusion with lysosomes, leading to a buildup of autophagic intermediates (16). This inhibition of autophagic flux allows for a better assessment of autophagic activity than any static time point as any proteins degraded by this process (*i.e.* LC3) will accumulate, permitting a more accurate quantitation of their turnover. Furthermore, we must note that LC3 and Beclin 1 are intermediates in converging lysosomal degradation pathways: LC3-associated phagocytosis, a process typically reserved for macrophages and a few other select cell types

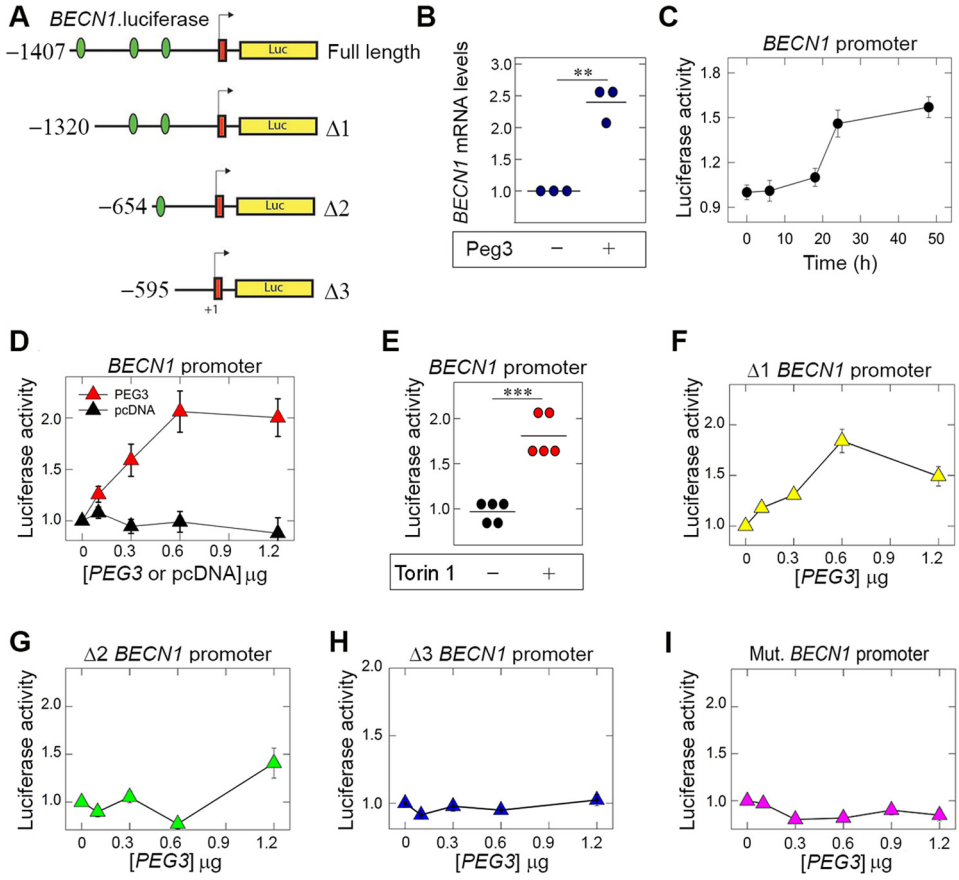

FIGURE 3. **Peg3 transcriptionally modulates *BECN1* activity.** *A*, full-length *BECN1* promoter containing three predicted binding sites (*green ovals*) and serial 5′ promoter truncations were inserted into a pGL3 Basic luciferase vector. *B*, effects of Peg3 expression on *BECN1* mRNA levels, normalized to *ACTB* mRNA. Values represent three independent trials performed in triplicate. *C*, time course of Peg3 transfections showing optimal luciferase activity of the full-length *BECN1* promoter at 48 h. *D–H*, representative luciferase reporter assays of PAER2 cells stably transfected with the indicated luciferase constructs and then transiently transfected for 48 h with the designated concentrations of Peg3, normalized to total protein. Significant values represent three independent trials performed in triplicate (***, $p < 0.001$; **, $p < 0.01$; *, $p < 0.05$ as compared with 0 ng of Peg3; Student's *t* test). Treatment of PAER2$^{BECN1\text{-}Luc}$ with the mTOR inhibitor Torin 1 was used as a positive control. *I*, *BECN1* promoter was synthesized by GenScript, incorporating nucleotide base changes, 5′-TGGCT-3′ to 5′-TAACC-3′, of the putative Peg3-binding site. The promoter region was inserted into a luciferase reporter construct and stably transfected into PAER2 cells. Transient transfection of Peg3 displayed no significant change in reporter activity (Student's *t* test; $p > 0.05$). Values represent three independent trials performed in triplicate. *Error bars* represent S.E. *Mut.*, mutant.

such as retinal pigment epithelial cells (79), and canonical autophagy. To determine which pathway was affected by Peg3, we tested the expression of FIP200, a specific autophagic marker (80). Indeed, we observed significant increases in FIP200 following Peg3 overexpression vis-à-vis empty vector in the presence of bafilomycin A1 (Fig. 5*A*), suggesting that Peg3 evokes turnover of FIP200. Thus, Peg3 specifically promotes canonical autophagy rather than LC3-associated phagocytosis.

During autophagy, LC3 is cleaved and conjugated with phosphatidylethanolamine to form LC3-II. This lipidated LC3-II associates with the outer membrane of the autophagosome and, as mentioned above, is itself degraded by the autophagic process. As such, it has been used as a reliable marker of autophagic flux (81, 82). PAER2^{PEG3} cells displayed a higher level of LC3-II as compared with cells transfected with empty vector (Fig. 5*B*, compare *lanes 1* and *5*). These cells also demonstrated more LC3-II in the presence of bafilomycin A1 (Fig. 5*B*, compare *lanes 5* and *6*), suggesting that the increase in LC3-II compared with PAER2^{pcDNA} in the absence of autophagic blockade was due to increased autophagic activity evoked by Peg3 overexpression. Importantly, treatment with bafilomycin A1 in conjunction with constitutive expression of Peg3 evoked a significant increase in LC3-II above that induced by bafilomycin A1 treatment alone ($p < 0.01$; Fig. 5*B*, compare *lanes 2* and *6*). Therefore, Peg3 increases LC3 turnover (and hence autophagic flux) beyond basal levels. This increase in LC3-II expression was similar to that seen with treatment of rapamycin in combination with bafilomycin A1.

Next, we used immunofluorescence to visualize autophagic flux. These findings mirrored the results seen at the biochemical level where PAER2$^{GFP\text{-}LC3}$ cells transfected with Peg3 showed an increase in LC3 puncta as compared with vehicle, similar to treatment with rapamycin (Fig. 5, *C–H*). Furthermore, more LC3-positive puncta were observed in cells overexpressing Peg3 compared with empty vector in the presence of bafilomycin A1, validating the hypothesis that Peg3 overexpression induces autophagic flux beyond levels seen in cells expressing endogenous Peg3.

To determine that Peg3 indeed utilizes the Beclin 1 pathway in the induction of autophagy, we silenced Beclin 1 using siRNA. Depletion of Beclin 1 in PAER2^{PEG3} cells abolished Peg3-driven autophagic flux (Fig. 5, *I*, *K*, and *N*) where Beclin

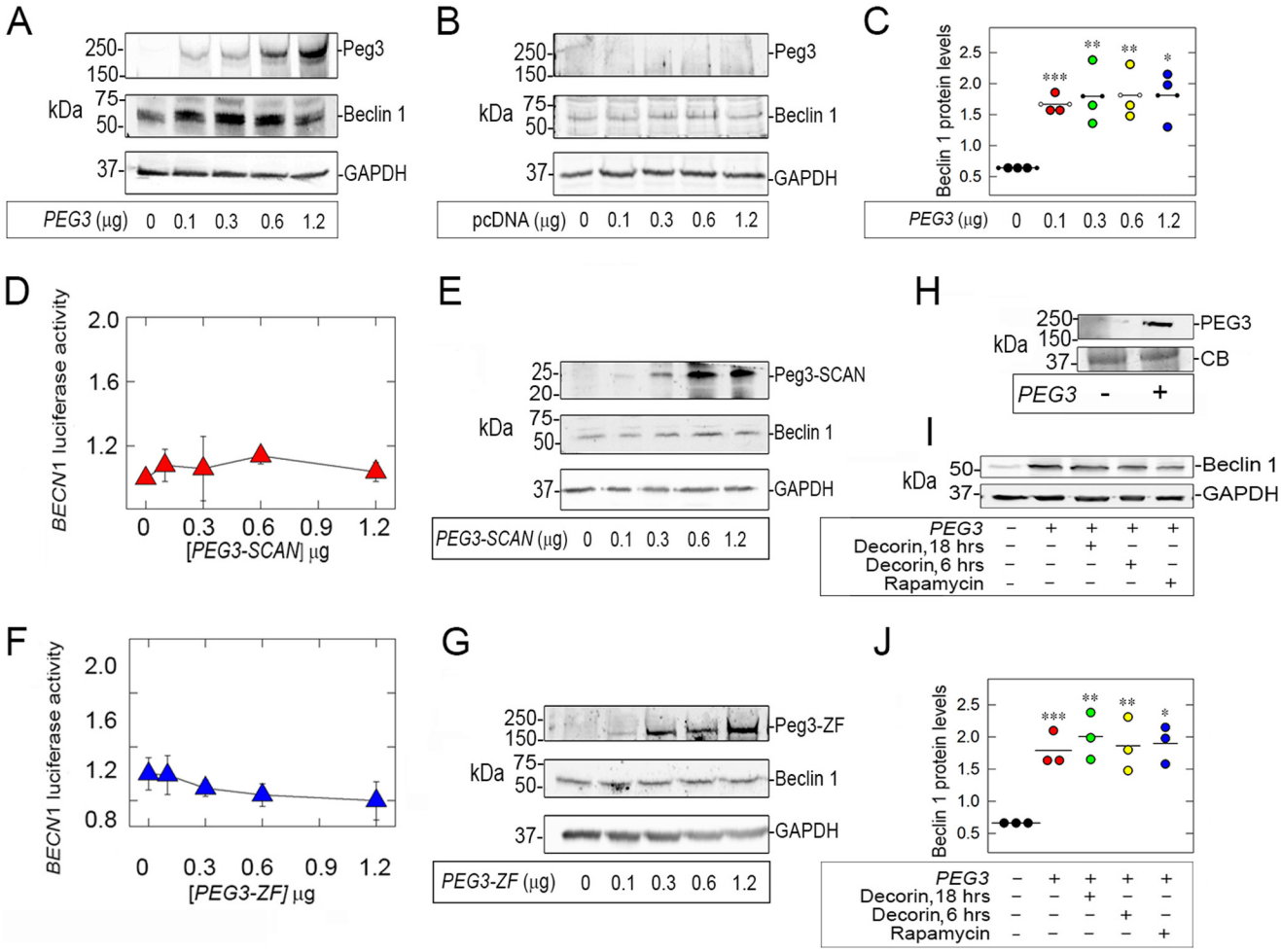

FIGURE 4. ***De novo* overexpression of full-length Peg3 is necessary for increased *BECN1* transcription and protein expression in endothelial cells.** *A–C*, Western blots of endothelial cell lysates to validate transfection efficiency. Notice the dose-dependent increase in Peg3 and concomitant induction of Beclin 1 (*A*) as compared with transfection with empty vector (*B*). *C*, quantification of three independent experiments performed in triplicate (Student's *t* test; ***, $p < 0.001$; **, $p < 0.0$; *, $p < 0.05$). *D* and *F*, cells transfected with truncated Peg3 for 48 h display no significant change in *BECN1* promoter activity, normalized to total protein. *E* and *G*, representative Western blots validating transfection efficiency of truncations and confirming no effect on Beclin 1 protein expression. *H*, confirmation of stable overexpression of Peg3. *I*, representative Western blot of Beclin 1 in stably expressing Peg3 cells following treatment with decorin (200 nM) or rapamycin (40 nM) for the designated time points. *J*, quantification of three independent experiments (Student's *t* test; ***, $p < 0.001$; **, $p < 0.01$; *, $p < 0.05$). *Error bars* represent S.E.

1-deficient PAER2^{PEG3} treated with bafilomycin A1 displayed no significant increase in LC3-positive puncta (Fig. 5, *I* and *K*) or LC3-II protein levels (Fig. 5, *M* and *N*) vis-à-vis PAER2^{PEG3}. Moreover, as a positive control, PAER2^{pcDNA} cells treated with rapamycin also displayed a decrease in autophagic flux when Beclin 1 was silenced (Fig. 5, *J*, *L*, *M*, and *N*). These data underscore the importance of the Peg3-Beclin 1 axis for competent autophagic flux and position Peg3 as a critical regulator of endothelial cell autophagy.

Peg3 Inhibits Endothelial Cell Motility and Emigration from a 3D Matrix—Both *in vivo* and *ex vivo* assays utilizing *Becn1*$^{+/-}$ mice demonstrated increased angiogenic activity relative to wild-type mice (83). Notably, endothelial cells derived from *Becn1*$^{+/-}$ mice display increased migration and tube formation, suggesting a link between Beclin 1 and regulation of angiogenesis. Therefore, we sought to determine whether overexpression of Peg3 would affect angiogenesis. In *in vitro* wound healing assays, endothelial cells stably expressing Peg3 were not able to close the wound as efficiently as compared with control cells expressing an empty vector (Fig. 6*A*). Indeed, PAER2^{pcDNA} displayed an approximately ~80% wound closure after 24 h, whereas PAER2^{PEG3} displayed only a ~25% wound closure after 24 h ($p < 0.001$; Fig. 6*B*).

To determine whether the inability of PAER2^{PEG3} cells to close the wound was due to a decrease in motility or a decrease in proliferation, we performed MTT proliferation assays. We found no significant change in proliferation between cell types over a period of 4 days (Fig. 6*C*), indicating that Peg3 affects primarily endothelial cell motility.

To expand and corroborate the results obtained in a 2D system, we performed emigration assays where endothelial cells stably expressing Peg3 or empty vector were embedded in a 3D matrix composed of growth factor-reduced Matrigel. Following 24 h, PAER2^{PEG3} cells had a markedly reduced number of cells that emigrated from the 3D matrix (Fig. 6*D*), and this was statistically significant ($p < 0.01$; Fig. 6*E*). Collectively, these data indicate that Peg3 inhibits endothelial cell motility in both 2D and 3D environments.

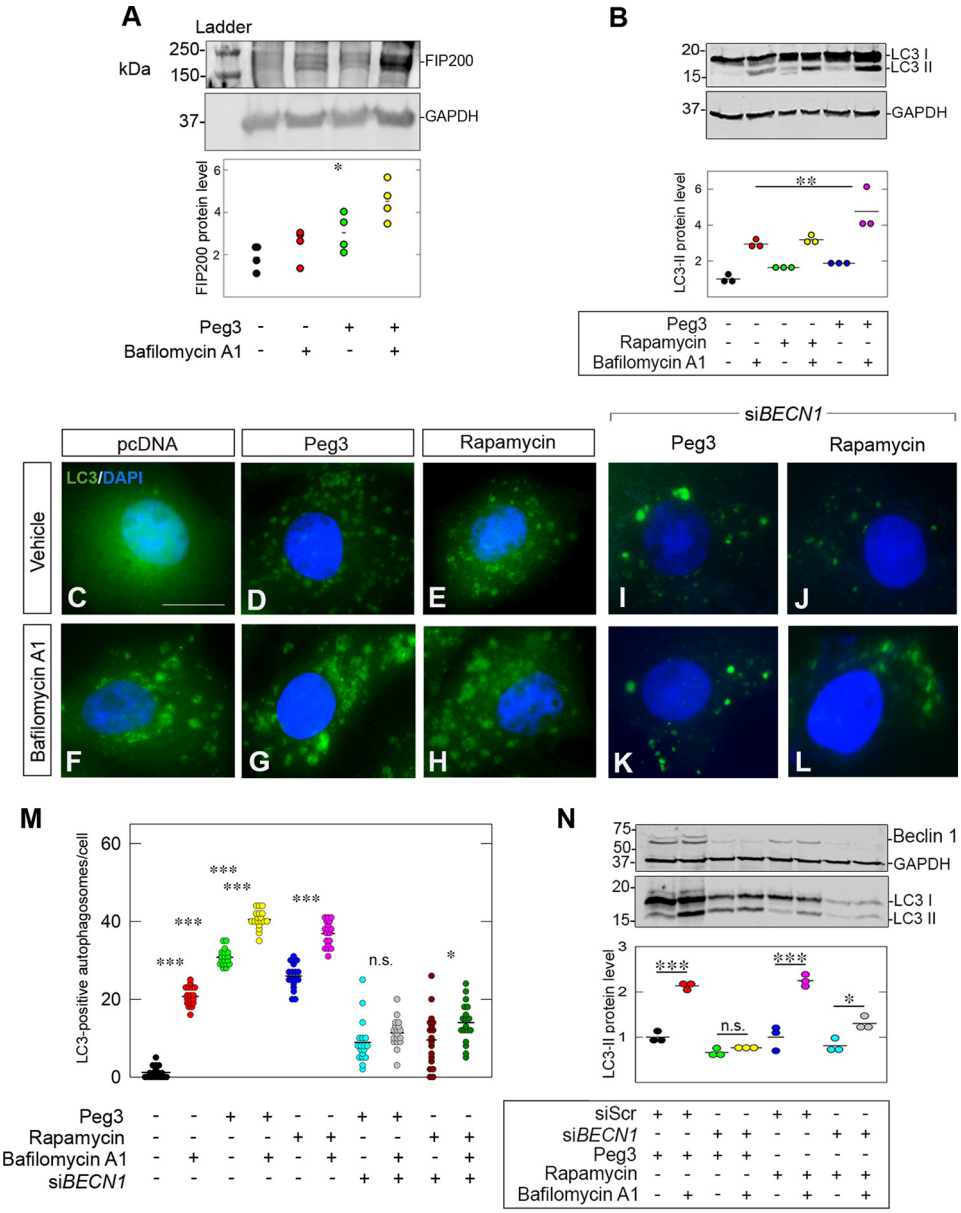

FIGURE 5. **Peg3 evokes Beclin 1-dependent autophagic flux.** *A*, representative Western blot of FIP200 following 6-h treatment with bafilomycin A1 (100 nM) of PAER2 cells stably transfected with either empty vector or Peg3. The Western blot is representative of four independent trials with similar results. Quantification of FIP200 shows statistical significance over empty vector control in the presence of bafilomycin A1 (Student's *t* test; *, $p < 0.05$). *B*, representative Western blot of LC3-II in PAER2^{pcDNA}, PAER2^{PEG3}, and PAER2^{pcDNA} treated with rapamycin (40 nM) in the absence and presence of bafilomycin A1. Quantification of three independent experiments shows significant increases in LC3-II protein with bafilomycin A1 treatment in the presence of Peg3 compared with empty vector (Student's *t* test; **, $p < 0.01$). *C–H*, immunofluorescence images of PAER2$^{GFP\text{-}LC3}$ cells transfected with the designated vectors showing LC3 (*green*) puncta in the absence and presence of bafilomycin A1. Rapamycin was used as a positive control. *I–L*, immunofluorescence images of Beclin 1-deficient PAER2$^{GFP\text{-}LC3}$ cells following Peg3 overexpression and rapamycin treatment (*scale bar*, ~10 μm). Images in *C–H* and *I–L* were obtained from separate experiments where each respective set of experiments utilized the same exposure, gain, and intensity. *M*, quantification of *C–L* (Student's *t* test; ***, $p < 0.001$; *, $p < 0.05$). *N*, biochemical analysis of LC3-II following Beclin 1 knockdown in cells overexpressing Peg3 or treated with rapamycin. Quantification is shown following three independent experiments (Student's *t* test; ***, $p < 0.001$; *, $p < 0.05$; *n.s.*, not significant).

Peg3 Alters the Secretome to Inhibit Endothelial Cell Motility—To examine whether the decrease in wound closure was due to secreted factors evoked by Peg3 overexpression, we performed scratch assays using media conditioned for 48 h by PAER2^{pcDNA} or PAER2^{PEG3} cells. PAER2^{pcDNA} cells incubated in their own conditioned media displayed an almost complete closure after 48 h, whereas PAER2^{pcDNA} cells incubated in media conditioned by PAER2^{PEG3} cells exhibited a significant reduction in wound closure at both 24 and 48 h (Fig. 7*A*). To provide a potential link to Peg3-mediated autophagy, treatment with rapamycin was utilized, which also inhibited wound closure to a similar extent as seen with the PAER2^{PEG3}-conditioned media ($p < 0.001$; Fig. 7*B*).

To further validate that secreted factors contributed to the decrease in wound closure in the PAER2^{PEG3} cells, we treated these cells with media conditioned by the PAER2^{pcDNA} cells. Indeed, we were able to partially rescue the inhibitory effect of media conditioned by PAER2^{PEG3} cells (Fig. 7*C*). After 48 h, there was a significant increase in wound closure when compared with PAER2^{PEG3} cells incubated in their own con-

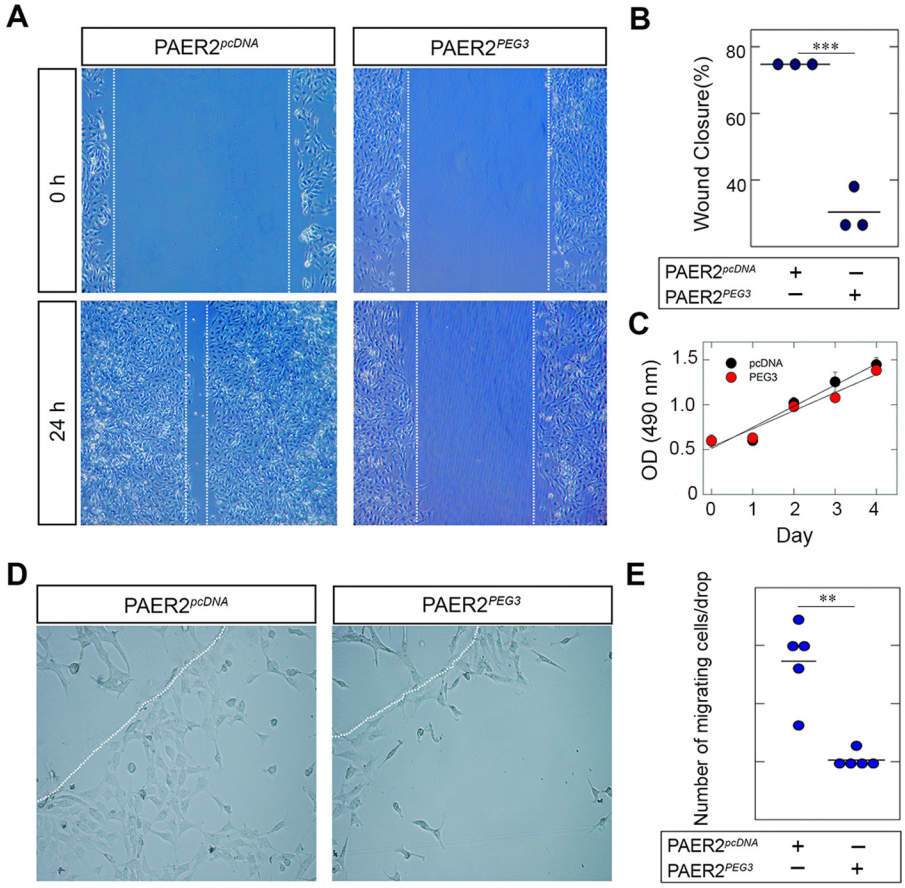

FIGURE 6. ***De novo* Peg3 expression attenuates wound healing and evasion from 2D and 3D matrices.** *A*, motility assays of PAER2 cells overexpressing Peg3 or empty vector. Monolayers were uniformly scratched to form a wound, and images were taken at 0 and 24 h. *B*, quantification of percent wound closure at 24 h as compared with zero time (Student's *t* test; $n = 3$ each; ***, $p < 0.001$). *C*, MTT proliferation assays performed between empty vector- and PEG3-expressing cells over a period of 4 days. Results are expressed as absorbance at 490 nm and represent triplicate measurements from at least three independent experiments. *D*, evasion of PAER2^{pcDNA} and PAER2^{PEG3} cells embedded in a Matrigel matrix. *Dotted white lines* outline the edge of the Matrigel drops. Images were captured at 24 h. *E*, quantification of cells migrated from each Matrigel drop. Data are of five independent experiments (Student's *t* test; **, $p < 0.01$). *Error bars* represent S.E.

ditioned media ($p < 0.001$; Fig. 7*D*). We conclude that Peg3 alters the endothelial cell secretome and may inhibit angiogenesis by modulating the secretion of antiangiogenic factors.

Peg3 Induces Thrombospondin 1 Secretion and Inhibits Capillary Morphogenesis Independently of Beclin 1—As decorin induces rapid Thrombospondin 1 (TSP-1) secretion in triple negative breast carcinoma cells (84), we hypothesized that the decorin-inducible Peg3 could be directly involved in stimulating the release and potential synthesis of TSP-1. This hypothesis was further strengthened by our close analysis of the *THBS1* promoter where we identified two putative Peg3-binding sites within a 3-kb promoter region. Notably, PAER2^{PEG3} cells had a significant increase ($p < 0.05$) in *THBS1* mRNA expression as compared with PAER2^{pcDNA} (Fig. 8*A*). Moreover, immunoblotting of media conditioned by Peg3-overexpressing endothelial cells showed enhanced TSP-1 secretion when normalized to cell number (Fig. 8*B*).

Next, we performed capillary morphogenesis assays in fibrillar collagen I using human umbilical vein endothelial cells (HUVECs). HUVECs incubated in media conditioned by PAER2^{pcDNA} cells formed capillary-like structures after 6 h; in contrast, HUVECs incubated in media conditioned by PAER2^{PEG3} failed to form tubes, further indicating that inhibition of capillary morphogenesis was due to an abundance of a secreted antiangiogenic factor (*e.g.* TSP-1) (Fig. 8*C*). Importantly, supplementing media conditioned by PAER2^{PEG3} with a TSP-1-blocking antibody partially rescued tube formation. Furthermore, media conditioned by PAER2^{pcDNA} treated with rh-TSP-1 abolished tube formation in HUVECs, mimicking the effects seen with the PAER2^{PEG3}-conditioned media (Fig. 8*D*). Quantitatively, there was a 4-fold suppression in the number of tubes formed when cells were incubated with PAER2^{PEG3}-conditioned media but significant tube formation when TSP-1 was blocked ($p < 0.001$; Fig. 8*E*).

Next, we determined whether the Peg3 induction of Beclin 1 was directly linked to the increase in TSP-1 secretion. Beclin 1 was knocked down in PAER2^{PEG3} cells using siRNA, and the media were collected after 48 h (Fig. 8*F*). To our great surprise, we found that the level of TSP-1 secretion was not altered, indicating that Beclin 1 had no effect on the already augmented secretion of basal TSP-1 as evoked by the *de novo* and stable expression of Peg3 (Fig. 8*F*).

These findings provide robust evidence that the inhibition of endothelial cell motility evoked by Peg3 is due to an alteration of the endothelial secretome independent of Beclin 1. Thus,

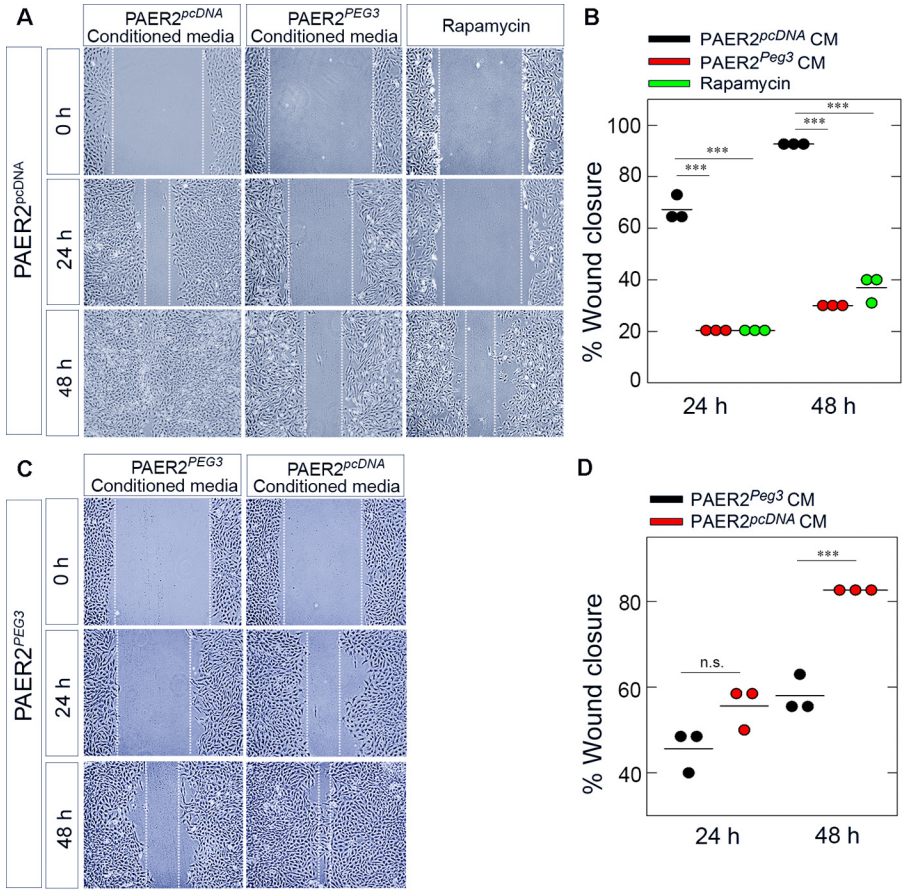

FIGURE 7. **Peg3 alters the secretome to inhibit wound healing.** *A*, motility assays of transgenic PAER2^{pcDNA} cells incubated with PAER^{PEG3}-conditioned media or treated with 40 nM rapamycin. *B*, quantification of percent wound closure after 24- and 48-h incubation with conditioned media (*CM*) or rapamycin as compared with time 0. Data represent three independent experiments (Student's *t* test; ***, $p < 0.001$). *C*, motility assay rescue experiments of PAER^{PEG3} cells incubated with PAER2^{pcDNA}-conditioned media. *D*, quantification of PAER2^{PEG3} cells incubated with conditioned media. Data represent three independent trials performed in triplicate (Student's *t* test; ***, $p < 0.001$; *n.s.*, not significant).

TSP-1 is a potent contributor to the antiangiogenic effect of Peg3.

Discussion

We provide the first evidence that an imprinted gene is capable of inducing autophagy, a highly conserved eukaryotic process that maintains cellular homeostasis (16). Previous studies have implicated an aberrant autophagic pathway in several diseases including cancer and neurodegenerative and myodegenerative diseases (85–89). Basal autophagy is particularly important in tissues where cells are non-proliferative such as neurons and myocytes. In such tissues, fine-tuned cytosolic turnover is necessary for survival, and interestingly, these are regions in which Peg3 is highly expressed (86, 90). Moreover, Peg3 is induced upon starvation, a condition that activates autophagy (91).

In cancer, autophagy plays a dual role: it can function as a tumor suppressor, inhibiting tumor initiation through clearance of misfolded proteins, reactive oxygen species, and other factors that contribute to genomic instability. However, it can promote tumor cell survival by enabling cancer cells to overcome high energy demands (92–94). Notably, reintroduction of Peg3 into glioma xenografts inhibits tumor growth, suggesting that Peg3 functions as a tumor suppressor. Other established tumor suppressor genes (*i.e.* p53, phosphatase and tensin homolog (PTEN), death-associated protein kinase, and tuberous sclerosis 1 and 2), which are also silenced in many cancers, are capable of stimulating autophagy (92). In fact, expression of the proautophagic protein Beclin 1 correlates with cancer prognosis where low levels are associated with a worse outcome in colorectal, pancreatic, gastric, and breast cancers and high levels of expression are associated with improved survival (95–97). Our data provide evidence that Peg3 modulates *BECN1* expression to evoke autophagy in endothelial cells. This may contribute to tumor growth inhibition by suppressing angiogenesis as well as by promoting autophagic cell death considering that Peg3 also functions downstream of p53 to induce apoptosis and these two pathways are interconnected (98). Furthermore, HUVECs treated with the angiogenesis inhibitor bortezomib undergo autophagic cell death (99).

Previous studies have shown that Peg3 is primarily localized to the nucleus where it regulates a subset of genes involved in development and differentiation (24, 30, 100). Breeding experiments using a Peg3 mutant mouse model have proven that Peg3 transcriptionally regulates placenta-specific genes in the brain and genes involved in lipid metabolism (101, 102). Under basal, unstimulated conditions, Peg3 is primarily located in the

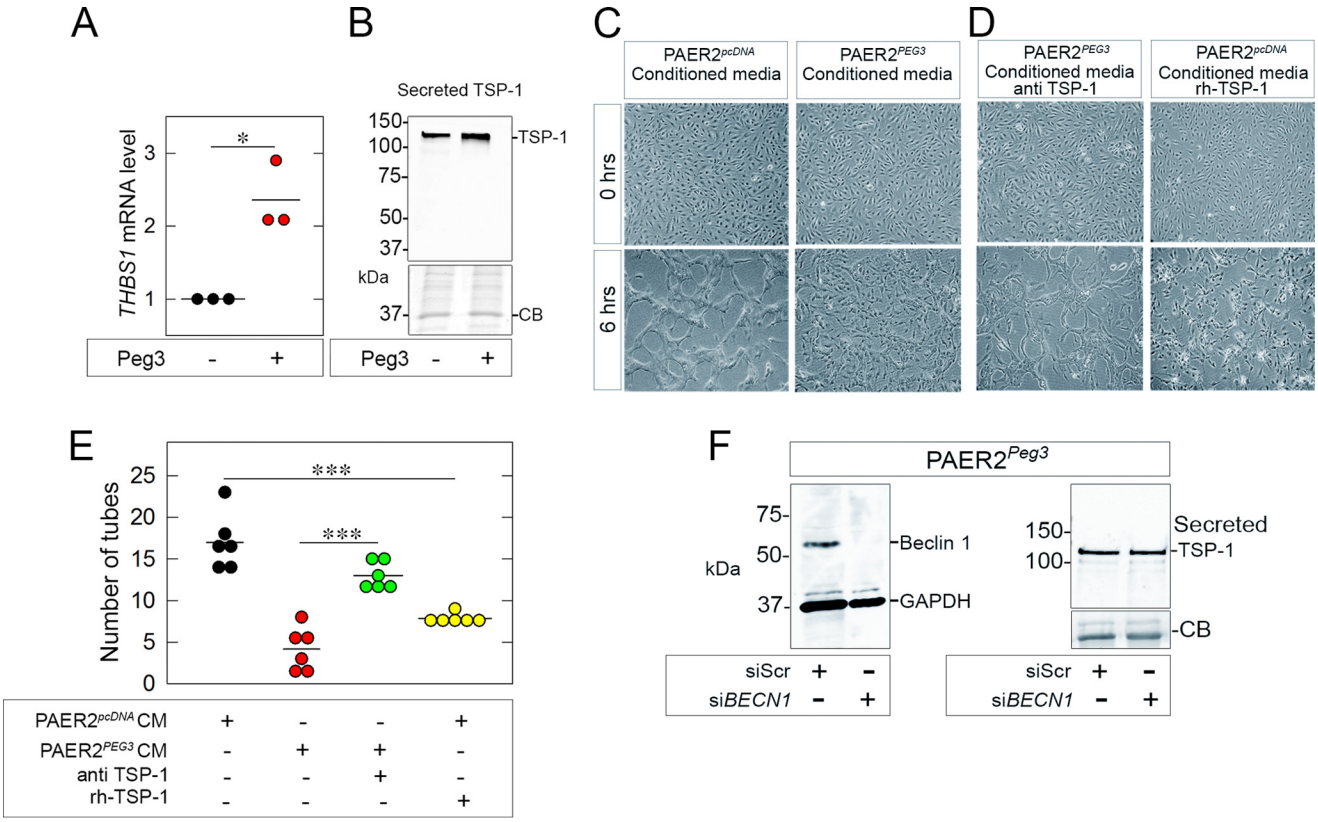

FIGURE 8. **Peg3 inhibits endothelial capillary morphogenesis via TSP-1 independently of Beclin 1.** *A*, PAER2^{PEG3} cells have increased *THBS1* mRNA levels, normalized to *ACTB* mRNA. Values represent three independent experiments performed in triplicate (Student's *t* test; *, $p < 0.05$). *B*, Western blot of 48-h conditioned media from stable cell lines displaying an increase of TSP-1 secretion with constitutive expression of Peg3, normalized to cell number. *C*, HUVECs incubated with conditioned media and coated with 1 mg/ml fibrillar collagen I gel to investigate capillary morphogenesis. *D*, capillary morphogenesis was rescued by the addition of an anti-TSP-1-blocking antibody to the PAER2^{PEG3}-conditioned media and inhibited by treatment with rh-TSP-1 (1 μg) added to the PAER2^{pcDNA}-conditioned media. *E*, quantification of the number of tubes formed per captured image of capillary morphogenesis assays. Data are of three independent trials (Student's *t* test; ***, $p < 0.001$). *F*, immunoblot displaying efficient knockdown of Beclin 1 in PAER2^{PEG3} cells using 100 pM si*BECN1*; scrambled siRNA (*siScr*) was used as a control. Knockdown of Beclin 1 had no effect on TSP-1 secretion by PAER2^{PEG3}. *CB*, Coomassie Blue; *CM*, conditioned media.

cytoplasm of endothelial cells (5). We expected that both the full length and the zinc finger-containing domain would translocate to the nucleus as both harbor a nuclear localization signal. Surprisingly, only the full-length Peg3 was capable of nuclear translocation. It is possible that the SCAN domain is necessary for specific protein-protein interactions that allow Peg3 to enter the nucleus.

In this study, we find that *BECN1* is a novel Peg3 target gene and identify a minimal promoter region between −1407 and −654 containing two Peg3-binding sites. The increase in *BECN1* transcription upon Peg3 overexpression is concomitant with the induction of protein levels of Beclin 1. Additionally, we present evidence that Peg3 directly modulates *BECN1* activity as mutation of putative Peg3-binding sites within the *BECN1* promoter region abolishes luciferase activity. Notably, in mouse brain, Peg3 can directly bind the promoter region of phosphoglucomutase 2-like 1 (*Pgm2l1*), the mouse homolog of glucose-1,6-biphosphate synthase, via the Peg3 binding motif. Thus, Peg3 is capable of directly binding DNA (76).

Endothelial cells stably expressing Peg3 display an increase in LC3-II, the lipidated form of LC3. This confirms our previous results that Peg3 functions within the PI3K/Akt/mTOR pathway (5). Importantly, treatment with bafilomycin A1 demonstrates that Peg3 induces autophagic flux. If autophagy induction by Peg3 were due to an inhibition of protein degradation, bafilomycin A1 treatment would have had no effect on LC3-II levels. Indeed, silencing Beclin 1 abrogates autophagic flux in Peg3 stably transfected cells, corroborating that Beclin 1 is necessary for Peg3-induced autophagy. Furthermore, although FIP200 has not yet been reported to be a substrate of autophagy, we show for the first time that Peg3-induced autophagy clears FIP200 in endothelial cells. This finding suggests new avenues of exploration for the nuances of Peg3-mediated autophagic control.

Inhibition of autophagy by knockdown of the autophagic gene *ATG7* has been shown to stimulate cell migration (103). It has also been demonstrated that decorin, an inducer of autophagy, is capable of blunting capillary morphogenesis and cell migration (51, 64) and interacting with various metalloproteinases (70) involved in modulating angiogenesis, wound repair, and fibrosis (34, 104–107). Recently, this ability of decorin to inhibit migration has been directly linked to its induction of autophagy (108). Peg3 functions downstream of decorin in the induction of autophagy in endothelial cells, and here we provide further evidence that Peg3 also blunts cell migration in both 2D and 3D environments. We must emphasize that Peg3 is positioned in an extracellularly regulated signaling axis where it is a direct downstream target of decorin and

endorepellin, two soluble matrix constituents that both halt angiogenesis by interfering with VEGFR2 (5, 9, 10, 109–112). Thus, there is a likely possibility of a connection among Peg3, autophagy, and angiogenesis.

Our study also provides mechanistic evidence that Peg3 inhibits motility and capillary morphogenesis by promoting the secretion of TSP-1, a powerful antiangiogenic factor (113–115). Although our aim was to connect TSP-1 secretion to Peg3-induced autophagy, we found that this secretion occurred independently of Beclin 1. We must reiterate, however, that there are Peg3-binding sites in the proximal region of the *THBS1* promoter suggesting that, like *BECN1*, *THBS1* may be a direct Peg3 target gene. Interestingly, activation of the TSP-1 receptor, CD47, induces autophagy in RAS-expressing cancer cells to quell tumor growth (116). Thus, it is possible that the Peg3-induced secretion of TSP-1 may be an indirect pathway through which Peg3 mediates Beclin 1 expression (potentially via CD47) and subsequently autophagy. This process could potentially explain why loss of Beclin 1 does not affect TSP-1 secretion. Paradoxically, other studies illustrate that blocking CD47 inhibits autophagy (117, 118), suggesting that Peg3-mediated TSP-1 secretion may also act as a feedback mechanism to maintain homeostasis under the highly autophagic conditions promoted by Peg3 overexpression. Regardless of the situation, the relationship between Peg3 and TSP-1 has an important implication in autophagic control in endothelial cells and is something to be investigated in future studies.

Although TSP-1 secretion is a partial mechanism for Peg3-mediated angiostasis, other secreted bioactive antiangiogenic and proautophagic factors may be at play as well. We hypothesize that top candidates may be endostatin and endorepellin, both of which are synthesized and secreted by endothelial cells (74, 84). In particular, both endostatin and endorepellin are known upstream effectors of Beclin 1 (9, 119), thereby providing a potential connection among Peg3, angiogenesis, and autophagy.

In conclusion, the ability for Peg3 to evoke a vital intracellular catabolic process in endothelial cells along with its alteration of the endothelial secretome, resulting in restricted migration and blunted capillary morphogenesis, underscores the importance of this decorin-induced gene in the regulation of endothelial cell homeostasis. Future work will likely elucidate the intricacies of Peg3 in angiostasis in terms of autophagic regulation. These findings are merely the beginning and should provide new avenues for better understanding angiogenesis in the context of cancer.

Experimental Procedures

Antibodies, Cells, and Reagents—The rabbit polyclonal antibodies against human lamin A/C, GAPDH, and Beclin 1 were from Cell Signaling Technology (Danvers, MA). Rabbit monoclonal antibody against the HA tag was also from Cell Signaling Technology. Peg3 antibody was custom made at GenScript. HRP-conjugated goat anti-rabbit secondary was from Millipore, Inc. (Billerica, MA) Donkey anti-rabbit secondary (Alexa Fluor 488) was from Life Technologies. SuperSignal West Pico chemiluminescence substrate was from Thermo Fisher Scientific (Philadelphia, PA). HUVECs were grown in basal medium supplemented with VascuLife EnGS LifeFactors kit (LifeLine Cell Technology, Frederick, MD) with cells being utilized within the first five passages. Transgenic porcine aortic endothelial cells expressing VEGFR2 were described previously (120). These cells were stably transfected with a luciferase reporter construct driven by a 1.4-kb region or fragments containing a 1.3-kb, 645-bp, or 595-bp region of the *BECN1* promoter linked to 514 bp of the first exon and a portion of the first intron of the *BECN1* gene. Cells were grown at 37 °C in a 5% CO_2 atmosphere in Dulbecco's modified Eagle's medium (DMEM) containing 4.5 g/liter glucose, L-glutamine, and sodium pyruvate from Life Technologies and supplemented with 10% fetal bovine serum (FBS) from Thermo Fisher Scientific and 100 units/ml penicillin/streptomycin from Life Technologies. Lipofectamine LTX and hygromycin B were from Invitrogen. Rapamycin was from Sigma-Aldrich.

Immunofluorescence and Confocal Microscopy—PAER2 cells ($\sim 5 \times 10^4$) were grown on coverslips coated with 0.2% gelatin. Cells were transfected with HA-PEG3, HA-SCAN, or HA-ZF for 48 h, then fixed with 4% paraformaldehyde at 4 °C, and permeabilized with 0.01% Triton X-100. Cell were blocked in 5% BSA in PBS, incubated with primary rabbit anti-HA antibody for 1 h at room temperature, and then incubated with donkey anti-rabbit Alexa Fluor 488 secondary antibody for 1 h. DAPI (Vector Laboratories) was used to visualize nuclei. Immunofluorescence and confocal (121–123) images were obtained as described previously (9).

Nuclear and Cytoplasmic Fractionation and Immunoblotting—Approximately 10^7 transfected cells were harvested and centrifuged at $500 \times g$ for 5 min. Cell pellets were washed in PBS, and fractionation was performed using NE-PER Nuclear and Cytoplasmic Extraction Reagents (Thermo Scientific). Nuclear pellets were washed twice with PBS to eliminate cytoplasmic contaminants before extraction. Following treatments, endothelial cells were lysed in radioimmune precipitation assay buffer (50 mM Tris-HCl, 50 mM NaCl, 1 mM EGTA, 1 mM EDTA, 1% Triton X-100, 0.5% sodium deoxycholate, 0.5% SDS, 1 mM sodium orthovanadate, 1 μg/ml leupeptin, 1 μg/ml aprotinin, 100 μM tosylphenylalanyl chloromethyl ketone, 1 mM PMSF, and one EDTA-free protease inhibitor tablet) for 20 min on ice. Proteins were separated by SDS-PAGE, transferred to nitrocellulose membrane (Bio-Rad), incubated with the appropriate antibodies, and visualized using enhanced chemiluminescence (Thermo Scientific) and an ImageQuant LAS 4000 (GE Healthcare).

Luciferase and Proliferation Assays—PAER2 cells were stably transfected with the indicated *BECN1*-luciferase constructs (primer sequences are listed in Table 1) and selected for 3 weeks with 500 μg of hygromycin B (Invitrogen). Mass cultures were collected and transiently transfected with increasing concentrations of Peg3 in 24-well plates. Luciferase was detected using a *Renilla* Luciferase Assay kit (Biotium) and measured using a plate luminometer (PerkinElmer Life Sciences). Data were normalized to total cell protein.

For cell proliferation assays, CellTiter Aqueous One Solution Cell Proliferation Assay was used (Promega). $PAER2^{pcDNA}$ and $PAER2^{PEG3}$ cells were seeded on 96-well microplates at a density of 5,000 cells/well in 100 μl of media. One Solution Reagent

TABLE 1
Primer sequences used for the construction of the indicated vectors
"F" denotes forward, and "R" denotes reverse.

Name	Primer sequence (5′ to 3′)
PEG3-SCAN	F, GCTAGCATGTACCATACGATGTTCCAGATTACGCTCTTCTGCCTCCAAAGCACTTG
	R, CTCGAGTGGTTGTACATCTCCTTGTAATTCCTCCAGCAGAGT
PEG3-ZF	F, GCTAGCATGTACCATACGATGTTCCAGATTACGCTCTTACGCAGGGCCACTCA
	R, GGATCCTCAGCCAGTGTGGGTATTCTGGTGTCTGGCGAGGGA
BECN1	F, GCTAGCTTTTGGGTTAAGCAGTGGTTTCTT
	R, CTCGAGTGAGGCCGTGGAAAAGAGGCAA
Δ1 BECN1	F, GCTAGCTTGGCTCACACCTGTAATCTCA
	R, CTCGAGTGAGGCCGTGGAAAAGAGGCAA
Δ3 BECN1	F, GCTAGCTGGTCTCGAACTCCTGACCTT
	R, CTCGAGTGAGGCCGTGGAAAAGAGGCAA

was added to the wells to be measured and incubated at 37 °C for 3 h each day for 4 days. Absorbance at 490 nm was recorded using a 96-well plate reader (PerkinElmer Life Sciences).

In Vitro Wound Healing, Matrigel Evasion, and Tube Formation Assays—For wound healing assays, PAER2 cells stably transfected with pcDNA or Peg3 were cultured on a 0.2% gelatin-coated 12-well dish. When cells reached subconfluence, scratches were made using a P-200 pipette tip. To evaluate the effect of conditioned media on wound healing, selected wells were incubated with 80% PAER2^{pcDNA} or PAER2^{PEG3} 48-h conditioned media. Tube formation assays were performed using HUVECs seeded on collagen-coated (100 μg/ml) 12-well dishes. After 24 h, 1 mg/ml fibrillar collagen (seven parts 1.4 mg/ml collagen, one part 10× medium 199, and two parts 11.8 mg/ml sodium bicarbonate) was placed on top of HUVECs and allowed to polymerize at 37 °C for 20 min. Conditioned media were placed over collagen gel, and select wells were treated with anti-Thrombospondin 1 (Santa Cruz Biotechnology) or rh-Thrombospondin 1 (R&D Systems) for 6 h. Conditioned media were collected after 48 h from confluent 10-cm dishes (10×10^6 cells) and filtered through a disposable 0.22-μm syringe-driven filter unit (Millipore). Images were taken using a digital microscope camera (Leica D-LUX3). For the evasion assay, the stable transfected endothelial cells used above were mixed in 1:2 ratios with Matrigel (BD Biosciences), and drops were placed at the corners of gelatin-coated chamber glass slides. Images were captured 24 h after incubation at 37 °C in basal medium (Lifeline Cell Technologies) with a digital epiluminescence microscope camera (CKX41, Olympus).

Real Time Gene Expression and Analysis—Stable cell lines PAER2^{pcDNA} and PAER2^{PEG3} were subjected to quantitative real time polymerase chain reaction (PCR) to confirm differences in *BECN1* and *THBS1* gene expression when Peg3 is constitutively expressed. Cells were lysed in 1 ml of TRIzol, and RNA was isolated using a Direct-zol RNA Miniprep kit (Zymo Research). Total RNA (1 μg) was annealed with oligo(dT) primers, and cDNA was synthesized using SuperScript Reverse Transcriptase II (Life Technologies). Gene-specific primer sets for *Sus scrofa* mRNA were designed for use in quantitative real time PCR. Target genes and endogenous housekeeping gene *ACTB* amplicons were amplified and analyzed as described previously (1).

siRNA-mediated Knockdown—Transient knockdown of Beclin 1 in PAER2^{PEG3} was achieved via 48-h transfection of siRNA specific for *S. scrofa* Beclin 1. Scrambled siRNA was used as a negative control. Two 10-cm dishes were seeded with PAER2^{PEG3} cells to achieve 80% confluence after attachment and transfected after 24 h with 100 pM scrambled siRNA or si*BECN1* and 10 μl of Lipofectamine RNAiMAX (Life Technologies) diluted in Opti-MEM medium (Gibco). Conditioned media were collected 48 h after transfection, and cells were lysed. Verification of siRNA-mediated knockdown was confirmed via Western blotting. Aliquots of conditioned media were analyzed by Western blotting to determine secreted levels of TSP-1 and normalized to cellular protein.

Author Contributions—R. V. I. and A. T. designed the study. R. V. I., A. T., and M. A. G. analyzed the data and wrote the manuscript. A. T. and M. A. G. performed the research.

Acknowledgments—We thank M. Johnson for providing the HA-tagged Peg3, L. Claesson-Welsh for providing the PAE-VEGFR2 cells, and F. Demarchi for providing the BECN1 promoter-luciferase construct. We thank all the members of the Iozzo laboratory for constructive criticisms during the course of these studies, especially T. Neill for critical reading of the manuscript. We also thank U. Rodeck, M. Pacifici, and J. Hoek for valuable advice.

References

1. Buraschi, S., Neill, T., Owens, R. T., Iniguez, L. A., Purkins, G., Vadigepalli, R., Evans, B., Schaefer, L., Peiper, S. C., Wang, Z. X., and Iozzo, R. V. (2012) Decorin protein core affects the global gene expression profile of the tumor microenvironment in a triple-negative orthotopic breast carcinoma xenograft model. *PLoS One* **7,** e45559
2. Iozzo, R. V., and Schaefer, L. (2015) Proteoglycan form and function: a comprehensive nomenclature of proteoglycans. *Matrix Biol.* **42,** 11–55
3. Neill, T., Schaefer, L., and Iozzo, R. V. (2015) Decoding the matrix: instructive roles of proteoglycan receptors. *Biochemistry* **54,** 4583–4598
4. Neill, T., Schaefer, L., and Iozzo, R. V. (2016) Decorin as a multivalent therapeutic agent against cancer. *Adv. Drug Deliv. Rev.* **97,** 174–185
5. Buraschi, S., Neill, T., Goyal, A., Poluzzi, C., Smythies, J., Owens, R. T., Schaefer, L., Torres, A., and Iozzo, R. V. (2013) Decorin causes autophagy in endothelial cells via Peg3. *Proc. Natl. Acad. Sci. U.S.A.* **110,** E2582–E2591
6. Goyal, A., Neill, T., Owens, R. T., Schaefer, L., and Iozzo, R. V. (2014) Decorin activates AMPK, an energy sensor kinase, to induce autophagy in endothelial cells. *Matrix Biol.* **34,** 46–54
7. Gubbiotti, M. A., Neill, T., Frey, H., Schaefer, L., and Iozzo, R. V. (2015) Decorin is an autophagy-inducible proteoglycan and is required for proper *in vivo* autophagy. *Matrix Biol.* **48,** 14–25
8. Gubbiotti, M. A., and Iozzo, R. V. (2015) Proteoglycans regulate autophagy via outside-in signaling: an emerging new concept. *Matrix Biol.* **48,** 6–13
9. Poluzzi, C., Casulli, J., Goyal, A., Mercer, T. J., Neill, T., and Iozzo, R. V. (2014) Endorepellin evokes autophagy in endothelial cells. *J. Biol. Chem.* **289,** 16114–16128

10. Goyal, A., Gubbiotti, M. A., Chery, D. R., Han, L., and Iozzo, R. V. (2016) Endorepellin-evoked autophagy contributes to angiostasis. *J. Biol. Chem.* **291,** 19245–19256
11. Bix, G., Fu, J., Gonzalez, E. M., Macro, L., Barker, A., Campbell, S., Zutter, M. M., Santoro, S. A., Kim, J. K., Höök, M., Reed, C. C., and Iozzo, R. V. (2004) Endorepellin causes endothelial cell disassembly of actin cytoskeleton and focal adhesions through the $\alpha 2\beta 1$ integrin. *J. Cell Biol.* **166,** 97–109
12. Bix, G., and Iozzo, R. V. (2005) Matrix revolutions: "tails" of basement-membrane components with angiostatic functions. *Trends Cell Biol.* **15,** 52–60
13. Iozzo, R. V. (2005) Basement membrane proteoglycans: from cellar to ceiling. *Nat. Rev. Mol. Cell Biol.* **6,** 646–656
14. Bix, G., Castello, R., Burrows, M., Zoeller, J. J., Weech, M., Iozzo, R. A., Cardi, C., Thakur, M. L., Barker, C. A., Camphausen, K., and Iozzo, R. V. (2006) Endorepellin *in vivo*: targeting the tumor vasculature and retarding cancer growth and metabolism. *J. Natl. Cancer Inst.* **98,** 1634–1646
15. Poluzzi, C., Iozzo, R. V., and Schaefer, L. (2016) Endostatin and endorepellin: a common route of action for similar angiostatic cancer avengers. *Adv. Drug Deliv. Rev.* **97,** 156–173
16. Levine, B., and Kroemer, G. (2008) Autophagy in the pathogenesis of disease. *Cell* **132,** 27–42
17. Lu, Y.-C., Song, J., Cho, H.-Y., Fan, G., Yokoyama, K. K., and Chiu, R. (2006) Cyclophilin A protects *Peg3* from hypermethylation and inactive histone modification. *J. Biol. Chem.* **281,** 39081–39087
18. O'Doherty, A. M., MacHugh, D. E., Spillane, C., and Magee, D. A. (2015) Genomic imprinting effects on complex traits in domesticated animal species. *Front. Genet.* **6,** 156
19. Rimsa, V., Eadsforth, T. C., and Hunter, W. N. (2013) Structure of the SCAN domain of human paternally expressed gene 3 protein. *PLoS One* **8,** e69538
20. Edelstein, L. C., and Collins, T. (2005) The SCAN domain family of zinc finger transcription factors. *Gene* **359,** 1–17
21. Kuroiwa, Y., Kaneko-Ishino, T., Kagitani, F., Kohda, T., Li, L.-L., Tada, M., Suzuki, R., Yokoyama, M., Shiroishi, T., Wakana, S., Barton, S. C., Ishino, F., and Surani, M. A. (1996) Peg3 imprinted gene on proximal chromosome 7 encodes for a zinc finger protein. *Nat. Genet.* **12,** 186–190
22. Relaix, F., Weng, X., Marazzi, G., Yang, E., Copeland, N., Jenkins, N., Spence, S. E., and Sassoon, D. (1996) Pw1, a novel zinc finger gene implicated in the myogenic and neuronal lineages. *Dev. Biol.* **177,** 383–396
23. Relaix, F., Wei, X. J., Wu, X., and Sassoon, D. A. (1998) Peg3/Pw1 is an imprinted gene involved in the TNF-NFκB signal transduction pathway. *Nat. Genet.* **18,** 287–291
24. Schwarzkopf, M., Coletti, D., Sassoon, D., and Marazzi, G. (2006) Muscle cachexia is regulated by a p53-PW1/Peg3-dependent pathway. *Genes Dev.* **20,** 3440–3452
25. Moresi, V., Pristerà, A., Scicchitano, B. M., Molinaro, M., Teodori, L., Sassoon, D., Adamo, S., and Coletti, D. (2008) Tumor necrosis factor-α inhibition of skeletal muscle regeneration is mediated by a caspase-dependent stem cell response. *Stem Cells* **26,** 997–1008
26. Besson, V., Smeriglio, P., Wegener, A., Relaix, F., Nait Oumesmar, B., Sassoon, D. A., and Marazzi, G. (2011) PW1 gene/paternally expressed gene 3 (PW1/Peg3) identifies multiple adult stem and progenitor cell populations. *Proc. Natl. Acad. Sci. U.S.A.* **108,** 11470–11475
27. Relaix, F., Wei, X. j., Li, W., Pan, J., Lin, Y., Bowtell, D. D., Sassoon, D. A., and Wu, X. (2000) Pw1/Peg3 is a potential cell death mediator and cooperates with Siah1a in p53-mediated apoptosis. *Proc. Natl. Acad. Sci. U.S.A.* **97,** 2105–2110
28. Deng, Y., and Wu, X. (2000) Peg3/Pw1 promotes p53-mediated apoptosis by inducing Bax translocation from cytosol to mitochondria. *Proc. Natl. Acad. Sci. U.S.A.* **97,** 12050–12055
29. Yamaguchi, A., Taniguchi, M., Hori, O., Ogawa, S., Tojo, N., Matsuoka, N., Miyake, S., Kasai, K., Sugimoto, H., Tamatani, M., Yamashita, T., and Tohyama, M. (2002) Peg3/Pw1 is involved in p53-mediated cell death pathway in brain ischemia/hypoxia. *J. Biol. Chem.* **277,** 623–629
30. Johnson, M. D., Wu, X., Aithmitti, N., and Morrison, R. S. (2002) Peg3/Pw1 is a mediator between p53 and Bax in DNA damage-induced neuronal death. *J. Biol. Chem.* **277,** 23000–23007
31. Champagne, F. A., Curley, J. P., Swaney, W. T., Hasen, N. S., and Keverne, E. B. (2009) Paternal influence on female behavior: the role of Peg3 in exploration, olfaction, and neuroendocrine regulation of maternal behavior of female mice. *Behav. Neurosci.* **123,** 469–480
32. Li, L., Keverne, E. B., Aparicio, S. A., Ishino, F., Barton, S. C., and Surani, M. A. (1999) Regulation of maternal behavior and offspring growth by paternally expressed *Peg3*. *Science* **284,** 330–333
33. Curley, J. P., Pinnock, S. B., Dickson, S. L., Thresher, R., Miyoshi, N., Surani, M. A., and Keverne, E. B. (2005) Increased body fat in mice with a targeted mutation of the paternally expressed imprinted gene *Peg3*. *FASEB J.* **19,** 1302–1304
34. Gaffney, J., Solomonov, I., Zehorai, E., and Sagi, I. (2015) Multilevel regulation of matrix metalloproteinases in tissue homeostasis indicates their molecular specificity *in vivo*. *Matrix Biol.* **44–46,** 191–199
35. Sengle, G., and Sakai, L. Y. (2015) The fibrillin microfibril scaffold: a niche for growth factors and mechanosensation? *Matrix Biol.* **47,** 3–12
36. Dowdy, S. C., Gostout, B. S., Shridhar, V., Wu, X., Smith, D. I., Podratz, K. C., and Jiang, S.-W. (2005) Biallelic methylation and silencing of paternally expressed gene 3 (*PEG3*) in gynecologic cancer cell lines. *Gynecol. Oncol.* **99,** 126–134
37. Feng, W., Marquez, R. T., Lu, Z., Liu, J., Lu, K. H., Issa, J.-P., Fishman, D. M., Yu, Y., and Bast, R. C., Jr. (2008) Imprinted tumor suppressor genes *ARHI* and *PEG3* are the most frequently down-regulated in human ovarian cancers by loss of heterozygosity and promoter methylation. *Cancer* **112,** 1489–1502
38. Maegawa, S., Yoshioka, H., Itaba, N., Kubota, N., Nishihara, S., Shirayoshi, Y., Nanba, E., and Oshimura, M. (2001) Epigenetic silencing of PEG3 gene expression in human glioma cell lines. *Mol. Carcinog.* **31,** 1–9
39. Song, J., Lu, Y., Giang, A., Pang, S., and Chiu, R. (2008) Promoter analysis of the mouse *Peg3* gene. *Biochim. Biophys. Acta* **1779,** 134–138
40. Nye, M. D., Hoyo, C., Huang, Z., Vidal, A. C., Wang, F., Overcash, F., Smith, J. S., Vasquez, B., Hernandez, B., Swai, B., Oneko, O., Mlay, P., Obure, J., Gammon, M. D., Bartlett, J. A., *et al.* (2013) Association between methylation of *paternally expressed gene* 3 (*PEG3*), cervical intraepithelial neoplasia and invasive cervical cancer. *PLoS One* **8,** e56325
41. Kohda, T., Asai, A., Kuroiwa, Y., Kobayashi, S., Aisaka, K., Nagashima, G., Yoshida, M. C., Kondo, Y., Kagiyama, N., Kirino, T., Kaneko-Ishino, T., and Ishino, F. (2001) Tumour suppressor activity of human imprinted gene *PEG3* in a glioma cell line. *Genes Cells* **6,** 237–247
42. Jiang, X., Yu, Y., Yang, H. W., Agar, N. Y., Frado, L., and Johnson, M. D. (2010) The imprinted gene *PEG3* inhibits Wnt signaling and regulates glioma growth. *J. Biol. Chem.* **285,** 8472–8480
43. Buraschi, S., Pal, N., Tyler-Rubinstein, N., Owens, R. T., Neill, T., and Iozzo, R. V. (2010) Decorin antagonizes Met receptor activity and down-regulates β-catenin and Myc levels. *J. Biol. Chem.* **285,** 42075–42085
44. Goldoni, S., Owens, R. T., McQuillan, D. J., Shriver, Z., Sasisekharan, R., Birk, D. E., Campbell, S., and Iozzo, R. V. (2004) Biologically active decorin is a monomer in solution. *J. Biol. Chem.* **279,** 6606–6612
45. Goldoni, S., and Iozzo, R. V. (2008) Tumor microenvironment: modulation by decorin and related molecules harboring leucine-rich tandem motifs. *Int. J. Cancer* **123,** 2473–2479
46. Frey, H., Schroeder, N., Manon-Jensen, T., Iozzo, R. V., and Schaefer, L. (2013) Biological interplay between proteoglycans and their innate immune receptors in inflammation. *FEBS J.* **280,** 2165–2179
47. Iozzo, R. V., and Schaefer, L. (2010) Proteoglycans in health and disease: novel regulatory signaling mechanisms evoked by the small leucine-rich proteoglycans. *FEBS J.* **277,** 3864–3875
48. Neill, T., Schaefer, L., and Iozzo, R. V. (2012) Decorin, a guardian from the matrix. *Am. J. Pathol.* **181,** 380–387
49. Rühland, C., Schönherr, E., Robenek, H., Hansen, U., Iozzo, R. V., Bruckner, P., and Seidler, D. G. (2007) The glycosaminoglycan chain of decorin plays an important role in collagen fibril formation at the early stages of fibrillogenesis. *FEBS J.* **274,** 4246–4255
50. Zhang, G., Chen, S., Goldoni, S., Calder, B. W., Simpson, H. C., Owens, R. T., McQuillan, D. J., Young, M. F., Iozzo, R. V., and Birk, D. E. (2009) Genetic evidence for the coordinated regulation of collagen fibrillogenesis in the cornea by decorin and biglycan. *J. Biol. Chem.* **284,** 8888–8897

51. Grant, D. S., Yenisey, C., Rose, R. W., Tootell, M., Santra, M., and Iozzo, R. V. (2002) Decorin suppresses tumor cell-mediated angiogenesis. *Oncogene* **21,** 4765–4777
52. Schönherr, E., Sunderkötter, C., Schaefer, L., Thanos, S., Grässel, S., Oldberg, A., Iozzo, R. V., Young, M. F., and Kresse, H. (2004) Decorin deficiency leads to impaired angiogenesis in injured mouse cornea. *J. Vasc. Res.* **41,** 499–508
53. Järveläinen, H., Puolakkainen, P., Pakkanen, S., Brown, E. L., Höök, M., Iozzo, R. V., Sage, E. H., and Wight, T. N. (2006) A role for decorin in cutaneous wound healing and angiogenesis. *Wound Repair Regen.* **14,** 443–452
54. Iozzo, R. V., Chakrani, F., Perrotti, D., McQuillan, D. J., Skorski, T., Calabretta, B., and Eichstetter, I. (1999) Cooperative action of germline mutations in decorin and p53 accelerates lymphoma tumorigenesis. *Proc. Natl. Acad. Sci. U.S.A.* **96,** 3092–3097
55. Häkkinen, L., Strassburger, S., Kähäri, V. M., Scott, P. G., Eichstetter, I., Lozzo, R. V., and Larjava, H. (2000) A role for decorin in the structural organization of periodontal ligament. *Lab. Invest.* **80,** 1869–1880
56. Robinson, P. S., Lin, T. W., Reynolds, P. R., Derwin, K. A., Iozzo, R. V., and Soslowsky, L. J. (2004) Strain-rate sensitive mechanical properties of tendon fascicles from mice with genetically engineered alterations in collagen and decorin. *J. Biomech. Eng.* **126,** 252–257
57. Ameye, L., and Young, M. F. (2002) Mice deficient in small leucine-rich proteoglycans: novel *in vivo* models for osteoporosis, osteoarthritis, Ehlers-Danlos syndrome, muscular dystrophy, and corneal diseases. *Glycobiology* **12,** 107R-116R
58. Nikitovic, D., Aggelidakis, J., Young, M. F., Iozzo, R. V., Karamanos, N. K., and Tzanakakis, G. N. (2012) The biology of small leucine-rich proteoglycans in bone pathophysiology. *J. Biol. Chem.* **287,** 33926–33933
59. Zoeller, J. J., Pimtong, W., Corby, H., Goldoni, S., Iozzo, A. E., Owens, R. T., Ho, S.-Y., and Iozzo, R. V. (2009) A central role for decorin during vertebrate convergent extension. *J. Biol. Chem.* **284,** 11728–11737
60. Morcavallo, A., Buraschi, S., Xu, S.-Q., Belfiore, A., Schaefer, L., Iozzo, R. V., and Morrione, A. (2014) Decorin differentially modulates the activity of insulin receptor isoform A ligands. *Matrix Biol.* **35,** 82–90
61. Nikolovska, K., Renke, J. K., Jungmann, O., Grobe, K., Iozzo, R. V., Zamfir, A. D., and Seidler, D. G. (2014) A decorin-deficient matrix affects skin chondroitin/dermatan sulfate levels and keratinocyte function. *Matrix Biol.* **35,** 91–102
62. Skandalis, S. S., Afratis, N., Smirlaki, G., Nikitovic, D., Theocharis, A. D., Tzanakakis, G. N., and Karamanos, N. K. (2014) Cross-talk between estradiol receptor and EGFR/IGF-IR signaling pathways in estrogen-responsive breast cancers: focus on the role and impact of proteoglycans. *Matrix Biol.* **35,** 182–193
63. Horváth, Z., Kovalszky, I., Fullár, A., Kiss, K., Schaff, Z., Iozzo, R. V., and Baghy, K. (2014) Decorin deficiency promotes hepatic carcinogenesis. *Matrix Biol.* **35,** 194–205
64. Järveläinen, H., Sainio, A., and Wight, T. N. (2015) Pivotal role for decorin in angiogenesis. *Matrix Biol.* **43,** 15–26
65. Danielson, K. G., Baribault, H., Holmes, D. F., Graham, H., Kadler, K. E., and Iozzo, R. V. (1997) Targeted disruption of decorin leads to abnormal collagen fibril morphology and skin fragility. *J. Cell Biol.* **136,** 729–743
66. Keene, D. R., San Antonio, J. D., Mayne, R., McQuillan, D. J., Sarris, G., Santoro, S. A., and Iozzo, R. V. (2000) Decorin binds near the C terminus of type I collagen. *J. Biol. Chem.* **275,** 21801–21804
67. Zhang, G., Ezura, Y., Chervoneva, I., Robinson, P. S., Beason, D. P., Carine, E. T., Soslowsky, L. J., Iozzo, R. V., and Birk, D. E. (2006) Decorin regulates assembly of collagen fibrils and acquisition of biomechanical properties during tendon development. *J. Cell. Biochem.* **98,** 1436–1449
68. Dunkman, A. A., Buckley, M. R., Mienaltowski, M. J., Adams, S. M., Thomas, S. J., Kumar, A., Beason, D. P., Iozzo, R. V., Birk, D. E., and Soslowsky, L. J. (2014) The injury response of aged tendons in the absence of biglycan and decorin. *Matrix Biol.* **35,** 232–238
69. Wu, Z., Horgan, C. E., Carr, O., Owens, R. T., Iozzo, R. V., and Lechner, B. E. (2014) Biglycan and decorin differentially regulate signaling in the fetal membranes. *Matrix Biol.* **35,** 266–275
70. Gubbiotti, M. A., Vallet, S. D., Ricard-Blum, S., and Iozzo, R. V. (2016) Decorin interacting network: a comprehensive analysis of decorin-binding partners and their versatile functions. *Matrix Biol.* **55,** 7–21
71. Reed, C. C., Gauldie, J., and Iozzo, R. V. (2002) Suppression of tumorigenicity by adenovirus-mediated gene transfer of decorin. *Oncogene* **21,** 3688–3695
72. Schaefer, L., and Iozzo, R. V. (2008) Biological functions of the small leucine-rich proteoglycans: from genetics to signal transduction. *J. Biol. Chem.* **283,** 21305–21309
73. Schaefer, L., and Iozzo, R. V. (2012) Small leucine-rich proteoglycans, at the crossroad of cancer growth and inflammation. *Curr. Opin. Genet. Dev.* **22,** 56–57
74. Neill, T., Painter, H., Buraschi, S., Owens, R. T., Lisanti, M. P., Schaefer, L., and Iozzo, R. V. (2012) Decorin antagonizes the angiogenic network. Concurrent inhibition of Met, hypoxia inducible factor-1α and vascular endothelial growth factor A and induction of thrombospondin-1 and TIMP3. *J. Biol. Chem.* **287,** 5492–5506
75. Yang, Z., and Klionsky, D. J. (2010) Eaten alive: a history of macroautophagy. *Nat. Cell Biol.* **12,** 814–822
76. Thiaville, M. M., Huang, J. M., Kim, H., Ekram, M. B., Roh, T.-Y., and Kim, J. (2013) DNA-binding motif and target genes of the imprinted transcription factor PEG3. *Gene* **512,** 314–320
77. Lee, S., Ye, A., and Kim, J. (2015) DNA-binding motif of the imprinted transcription factor PEG3. *PLoS One* **10,** e0145531
78. Thoreen, C. C., Kang, S. A., Chang, J. W., Liu, Q., Zhang, J., Gao, Y., Reichling, L. J., Sim, T., Sabatini, D. M., and Gray, N. S. (2009) An ATP-competitive mammalian target of rapamycin inhibitor reveals rapamycin-resistant functions of mTORC1. *J. Biol. Chem.* **284,** 8023–8032
79. Green, D. R., Oguin, T. H., and Martinez, J. (2016) The clearance of dying cells: table for two. *Cell Death Differ.* **23,** 915–926
80. Klionsky, D. J., Abdelmohsen, K., Abe, A., Abedin, M. J., Abeliovich, H., Acevedo Arozena, A., Adachi, H., Adams, C. M., Adams, P. D., Adeli, K., Adhihetty, P. J., Adler, S. G., Agam, G., Agarwal, R., Aghi, M. K., *et al.* (2016) Guidelines for the use and interpretation of assays for monitoring autophagy (3rd edition). *Autophagy* **12,** 1–222
81. Mizushima, N., Yoshimori, T., and Levine, B. (2010) Methods in mammalian autophagy research. *Cell* **140,** 313–326
82. Mizushima, N., and Yoshimori, T. (2007) How to interpret LC3 immunoblotting. *Autophagy* **3,** 542–545
83. Lee, S.-J., Kim, H. P., Jin, Y., Choi, A. M., and Ryter, S. W. (2011) Beclin 1 deficiency is associated with increased hypoxia-induced angiogenesis. *Autophagy* **7,** 829–839
84. Neill, T., Jones, H. R., Crane-Smith, Z., Owens, R. T., Schaefer, L., and Iozzo, R. V. (2013) Decorin induces rapid secretion of thrombospondin-1 in basal breast carcinoma cells via inhibition of Ras homolog gene family, member A/Rho-associated coiled-coil containing protein kinase 1. *FEBS J.* **280,** 2353–2368
85. Choi, A. M., Ryter, S. W., and Levine, B. (2013) Autophagy in human health and disease. *New Engl. J. Med.* **368,** 651–662
86. Ravikumar, B., Sarkar, S., Davies, J. E., Futter, M., Garcia-Arencibia, M., Green-Thompson, Z. W., Jimenez-Sanchez, M., Korolchuk, V. I., Lichtenberg, M., Luo, S., Massey, D. C., Menzies, F. M., Moreau, K., Narayanan, U., Renna, M., *et al.* (2010) Regulation of mammalian autophagy in physiology and pathophysiology. *Physiol. Rev.* **90,** 1383–1435
87. Grumati, P., and Bonaldo, P. (2012) Autophagy in skeletal muscle homeostasis and in muscular dystrophies. *Cells* **1,** 325–345
88. Custer, S. K., and Androphy, E. J. (2014) Autophagy dysregulation in cell culture and animals models of spinal muscular atrophy. *Mol. Cell. Neurosci.* **61,** 133–140
89. Menzies, F. M., Fleming, A., and Rubinsztein, D. C. (2015) Compromised autophagy and neurodegenerative diseases. *Nat. Rev. Neurosci.* **16,** 345–357
90. Hara, T., Nakamura, K., Matsui, M., Yamamoto, A., Nakahara, Y., Suzuki-Migishima, R., Yokoyama, M., Mishima, K., Saito, I., Okano, H., and Mizushima, N. (2006) Suppression of basal autophagy in neural cells causes neurodegenerative disease in mice. *Nature* **441,** 885–889
91. Ebert, S. M., Monteys, A. M., Fox, D. K., Bongers, K. S., Shields, B. E., Malmberg, S. E., Davidson, B. L., Suneja, M., and Adams, C. M. (2010) The transcription factor ATF4 promotes skeletal myofiber atrophy during fasting. *Mol. Endocrinol.* **24,** 790–799

92. Botti, J., Djavaheri-Mergny, M., Pilatte, Y., and Codogno, P. (2006) Autophagy signaling and the cogwheels of cancer. *Autophagy* **2,** 67–73
93. Degenhardt, K., Mathew, R., Beaudoin, B., Bray, K., Anderson, D., Chen, G., Mukherjee, C., Shi, Y., Gélinas, C., Fan, Y., Nelson, D. A., Jin, S., and White, E. (2006) Autophagy promotes tumor cell survival and restricts necrosis, inflammation, and tumorigenesis. *Cancer Cell* **10,** 51–64
94. Koren, I., and Kimchi, A. (2012) Promoting tumorigenesis by suppressing autophagy. *Science* **338,** 889–890
95. Yoo, B. H., Wu, X., Li, Y., Haniff, M., Sasazuki, T., Shirasawa, S., Eskelinen, E.-L., and Rosen, K. V. (2010) Oncogenic *ras*-induced down-regulation of autophagy mediator Beclin-1 is required for malignant transformation of intestinal epithelial cells. *J. Biol. Chem.* **285,** 5438–5449
96. Li, B.-X., Li, C.-Y., Peng, R.-Q., Wu, X.-J., Wang, H.-Y., Wan, D.-S., Zhu, X.-F., and Zhang, X.-S. (2009) The expression of *beclin* 1 is associated with favorable prognosis in stage IIIB colon cancers. *Autophagy* **5,** 303–306
97. Liang, X. H., Jackson, S., Seaman, M., Brown, K., Kempkes, B., Hibshoosh, H., and Levine, B. (1999) Induction of autophagy and inhibition of tumorigenesis by *beclin* 1. *Nature* **402,** 672–676
98. Nguygen, T. M., Subramanian, I. V., Kelekar, A., and Ramakrishnan, S. (2007) Kringle 5 of human plasminogen, an angiogenesis inhibitor, induces both autophagy and apoptotic death in endothelial cells. *Blood* **109,** 4793–4802
99. Belloni, D., Veschini, L., Foglieni, C., Dell'Antonio, G., Caligaris-Cappio, F., Ferrarini, M., and Ferrero, E. (2010) Bortezomib induces autophagic death in proliferating human endothelial cells. *Exp. Cell Res.* **316,** 1010–1018
100. Flisikowski, K., Venhoranta, H., Nowacka-Woszuk, J., McKay, S. D., Flyckt, A., Taponen, J., Schnabel, R., Schwarzenbacher, H., Szczerbal, I., Lohi, H., Fries, R., Taylor, J. F., Switonski, M., and Andersson, M. (2010) A novel mutation in the maternally imprinted *PEG3* domain results in a loss of *MIMT1* expression and causes abortions and stillbirths in cattle (*Bos taurus*). *PLoS One* **5,** e15116
101. Kim, J., Frey, W. D., He, H., Kim, H., Ekram, M. B., Bakshi, A., Faisal, M., Perera, B. P., Ye, A., and Teruyama, R. (2013) Peg3 mutational effects on reproduction and placenta-specific gene families. *PLoS One* **8,** e83359
102. Zhou, Q. Y., Li, C. C., Huo, J. H., and Zhao, S. H. (2011) Expression and genomic imprinting of *DCN*, *PON2* and *PEG3* genes in porcine placenta. *Anim. Reprod. Sci.* **123,** 70–74
103. Ramakrishnan, S., Nguygen, T. M., Subramanian, I. V., and Kelekar, A. (2007) Autophagy and angiogenesis inhibition. *Autophagy* **3,** 512–515
104. Deryugina, E. I., and Quigley, J. P. (2015) Tumor angiogenesis: MMP-mediated induction of intravasation- and metastasis-sustaining neovasculature. *Matrix Biol.* **44–46,** 94–112
105. Rohani, M. G., and Parks, W. C. (2015) Matrix remodeling by MMPs during wound repair. *Matrix Biol.* **44–46,** 113–121, 10.1016/j.matbio.2015.03.002
106. Itoh, Y. (2015) Membrane-type matrix metalloproteinases: their functions and regulations. *Matrix Biol.* **44–46,** 207–223
107. Duarte, S., Baber, J., Fujii, T., and Coito, A. J. (2015) Matrix metalloproteinases in liver injury, repair and fibrosis. *Matrix Biol.* **44–46,** 147–156
108. Yao, T., Zhang, C. G., Gong, M. T., Zhang, M., Wang, L., and Ding, W. (2016) Decorin-mediated inhibition of the migration of U87MG glioma cells involves activation of autophagy and suppression of TGF-β signaling. *FEBS Open. Bio* **6,** 707–719
109. Mongiat, M., Sweeney, S. M., San Antonio, J. D., Fu, J., and Iozzo, R. V. (2003) Endorepellin, a novel inhibitor of angiogenesis derived from the C terminus of perlecan. *J. Biol. Chem.* **278,** 4238–4249
110. Zoeller, J. J., and Iozzo, R. V. (2008) Proteomic profiling of endorepellin angiostatic activity on human endothelial cells. *Proteome Sci.* **6,** 7
111. Goyal, A., Poluzzi, C., Willis, C. D., Smythies, J., Shellard, A., Neill, T., and Iozzo, R. V. (2012) Endorepellin affects angiogenesis by antagonizing diverse VEGFR2-evoked signaling pathways: transcriptional repression of HIF-1α and VEGFA and concurrent inhibition of NFAT1 activation. *J. Biol. Chem.* **287,** 43543–43556
112. Willis, C. D., Poluzzi, C., Mongiat, M., and Iozzo, R. V. (2013) Endorepellin laminin-like globular repeat 1/2 domains bind Ig3–5 of vascular endothelial growth factor (VEGF) receptor 2 and block pro-angiogenic signaling by VEGFA in endothelial cells. *FEBS J.* **280,** 2271–2284
113. Murphy-Ullrich, J. E., and Sage, E. H. (2014) Revisiting the matricellular concept. *Matrix Biol.* **37,** 1–14
114. Stenina-Adognravi, O. (2014) Invoking the power of thrombospondins: regulation of thrombospondins expression. *Matrix Biol.* **37,** 69–82
115. Armstrong, L. C., and Bornstein, P. (2003) Thrombospondins 1 and 2 function as inhibitors of angiogenesis. *Matrix Biol.* **22,** 63–71
116. Kalas, W., Swiderek, E., Switalska, M., Wietrzyk, J., Rak, J., and Strzadala, L. (2013) Thrombospondin-1 receptor mediates autophagy of RAS-expressing cancer cells and triggers tumour growth inhibition. *Anticancer Res.* **33,** 1429–1438
117. Soto-Pantoja, D. R., Ridnour, L. A., Wink, D. A., and Roberts, D. D. (2013) Blockade of CD47 increases survival of mice exposed to lethal total body irradiation. *Sci. Rep.* **3,** 1038
118. Soto-Pantoja, D. R., Miller, T. W., Pendrak, M. L., DeGraff, W. G., Sullivan, C., Ridnour, L. A., Abu-Asab, M., Wink, D. A., Tsokos, M., and Roberts, D. D. (2012) CD47 deficiency confers cell and tissue radioprotection by activation of autophagy. *Autophagy* **8,** 1628–1642
119. Nguyen, T. M., Subramanian, I. V., Xiao, X., Ghosh, G., Nguyen, P., Kelekar, A., and Ramakrishnan, S. (2009) Endostatin induces autophagy in endothelial cells by modulating Beclin 1 and β-catenin levels. *J. Cell. Mol. Med.* **13,** 3687–3698
120. Goyal, A., Pal, N., Concannon, M., Paul, M., Doran, M., Poluzzi, C., Sekiguchi, K., Whitelock, J. M., Neill, T., and Iozzo, R. V. (2011) Endorepellin, the angiostatic module of perlecan, interacts with both the $\alpha2\beta1$ integrin and vascular endothelial growth factor receptor 2 (VEGFR2). *J. Biol. Chem.* **286,** 25947–25962
121. Rudnicka, L., Varga, J., Christiano, A. M., Iozzo, R. V., Jimenez, S. A., and Uitto, J. (1994) Elevated expression of type VII collagen in the skin of patients with systemic sclerosis. *J. Clin. Investig.* **93,** 1709–1715
122. Ryynänen, M., Ryynänen, J., Sollberg, S., Iozzo, R. V., Knowlton, R. G., and Uitto, J. (1992) Genetic linkage of Type VII collagen (COL7A1) to dominant dystrophic epidermolysis bullosa in families with abnormal anchoring fibrils. *J. Clin. Investig.* **89,** 974–980
123. Gonzalez, E. M., Mongiat, M., Slater, S. J., Baffa, R., and Iozzo, R. V. (2003) A novel interaction between perlecan protein core and progranulin: potential effects on tumor growth. *J. Biol. Chem.* **278,** 38113–38116